Cretaceous Research 110 (2020) 104414

Contents lists available at ScienceDirect

Cretaceous Research

journal homepage: www.elsevier.com/locate/CretRes

A Cenomanian–Santonian rudist–bearing carbonate platform on the northern Arabian Plate, Turkey: facies and sequence stratigraphy

Oğuz Mülayim [a, *], İsmail Ömer Yılmaz [b], Sacit Özer [c], Bilal Sarı [d], Kemal Taslı [e]

[a] TPAO, Turkish Petroleum Corporation, Adıyaman Directorate, Adıyaman, 02040, Turkey
[b] Middle East Technical University, Department of Geological Engineering, Ankara, 06800, Turkey
[c] 6349 Sok. 9/7, Atakent–Karşıyaka, İzmir, 35540, Turkey
[d] Dokuz Eylül University, Department of Geological Engineering, Buca, İzmir, 35370, Turkey
[e] Mersin University, Department of Geological Engineering, Mersin, 33342, Turkey

ARTICLE INFO

Article history:
Received 10 September 2019
Received in revised form
5 January 2020
Accepted in revised form 5 February 2020
Available online 11 February 2020

Keywords:
Cenomanian–Santonian
Carbonate ramp
Bivalves
Mediterranean

ABSTRACT

Recent studies have shown that Cenomanian–Santonian carbonate sedimentary rocks rich in rudists are widespread throughout southeastern Turkey. The Derdere and Karababa formations have been analysed in the Sabunsuyu section (Kilis Province). On a field scale, we can distinguish rudist–rich beds that rhythmically alternate with bioclastic levels composed of bivalves, gastropods and roveacrinids in these formations. Although pelagic faunal elements (predominantly planktic foraminifera and pithonellids) are documented in the lowermost part of the series, the rudist–rich facies are represented mainly in the Derdere and Karababa formations. Rudists, benthic and planktic foraminifera indicate middle–late Cenomanian and Turonian–Santonian ages for the Derdere and Karababa formations, respectively. Based on studied facies, five microfacies have been recognised and categorised in three facies groups: inner ramp, mid ramp and outer ramp. Evidence such as gradual changes in facies and absence of extensive uninterrupted barrier reefs indicate that the Derdere Formation was deposited in a ramp depositional system. The sedimentology and taphonomic signature of the rudist shell beds have been described in order to obtain a better understanding of the depositional environment and the physical processes that controlled Cenomanian–Santonian sedimentation. Monospecific tabular beds characterise mainly the upper part of the series (topmost part of Derdere Formation and Karababa Formation); more complex rudist concentrations, characterised by moderate species diversity, increase upsection. The rudist levels are associated with highstand systems tract deposits because of the suitability of trophic conditions in the rudist–dominated ramp.

1. Introduction

Rudist beds are widely exposed in Cenomanian to Maastrichtian (Upper Cretaceous) formations of the Arabian Platform (Steuber, 2002; Özer and Ahmad, 2015, 2016; Khazaei et al., 2010; Özer and El–Sorogy, 2017; Özer et al., 2013, 2019a). However, the taxonomic studies of rudists mainly focus on the uppermost Campanian–Maastrichtian in southeast Turkey (Steuber, 2002; Özer, 2005, 2010a, b; Özer et al., 2009; Steuber et al., 2009; Tunis et al., 2013), which is located in the northern part of the Arabian Platform. Although previous studies have hinted at the presence of rudist fragments in the Upper Cretaceous Derdere and Karababa formations in southeast Turkey, the rudist fauna has never been described in detail. Our recent studies have shown that the Cenomanian–Santonian formations (Derdere and Karababa) yield well–identifiable rudists that are of biostratigraphical importance in the Sabunsuyu section of the Kilis area (Fig. 1), although few rudist fragments have also been reported from these formations along the eastern side of the road, and upstream, in the area of the western Kilis by Keskin et al. (1974), Görür et al. (1981), Cros et al. (1999) and Gül et al. (2001).

The Cenomanian–Santonian succession is well exposed in the Sabunsuyu area and contains diverse macro– and microfaunas. Thus, the Sabunsuyu section is an ideal succession for establishing a reliable chronostratigraphy for southeast Turkey as a basis for comparisons and correlations with surrounding areas. The objective of the present work is to provide a stratigraphical,

* Corresponding author.
E-mail address: omulayim@tpao.gov.tr (O. Mülayim).

https://doi.org/10.1016/j.cretres.2020.104414
0195-6671/

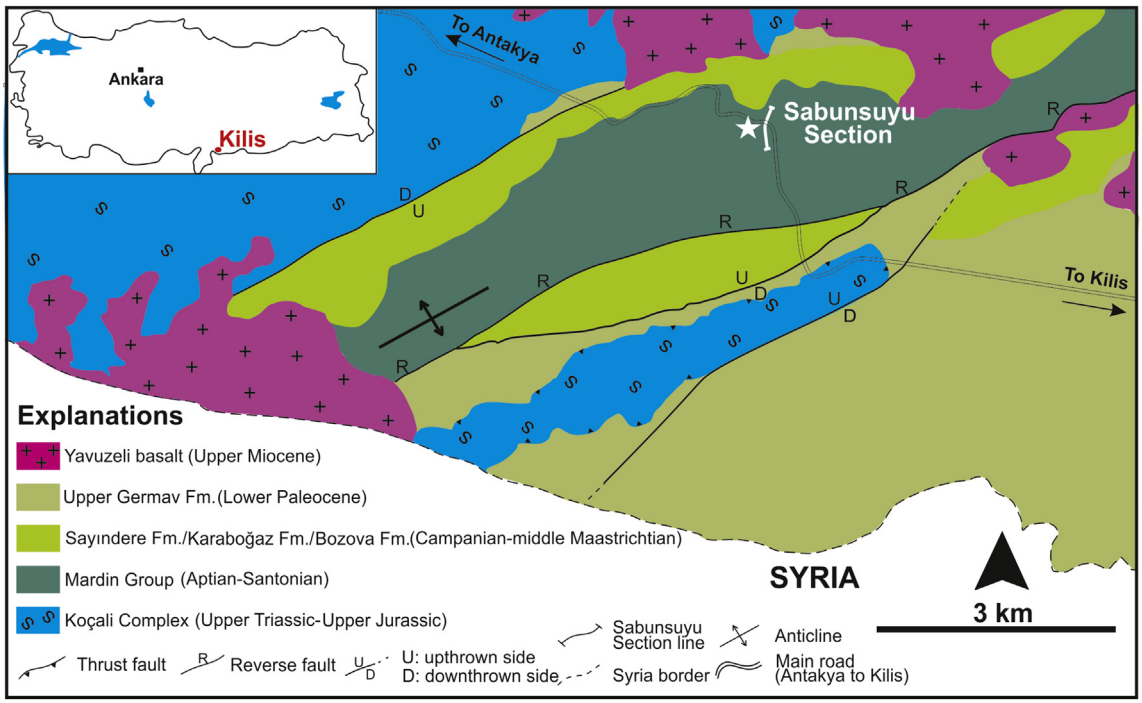

Fig. 1. Location map of the study area and geological map (modified from Aksu et al., 2014), showing the Sabunsuyu section.

facies analysis and sequence–stratigraphical study of the Cenomanian–Santonian succession exposed in the western of part of the Kilis area (southeast Turkey). Rudist associations of the Derdere and Karababa formations are documented to allow comparisons with those of the Arabian Platform. Macro– and microfacies analyses of the shallow– to deeper–water carbonates, which dominate the Cenomanian–Santonian succession, are supplied in order to obtain information on the depositional environment.

2. Material and methods

The Sabunsuyu section is located in the western part of the province of Kilis (co–ordinates 36.829233°/36.893509°). At this locality, the Cenomanian–Santonian succession has been measured in the Derdere and Karababa formations. The sampling of metre– to decimetre–scale for each bed in this Cenomanian–Santonian section has been made along the eastern side of the road and upstream. Rudists are mostly embedded in tightly packed limestones of the Derdere Formation. Therefore, we have used mainly field photographs for the description of rudists that show characteristic features of species and limestone samples displaying rudist sections, collected from the Sabunsuyu area. We have studied thin sections of 97 limestone samples collected throughout the stratigraphical section to describe both microfacies characteristics and microfossils. The descriptive taxonomy of all macro– and micropalaeontological taxa will be presented in detail in separate papers.

A detailed microfacies analysis of the succession was the main tool used in the present research for palaeoenvironmental interpretations. Palaeontological and petrographical components of 97 thin sections were studied by following the guidelines of carbonate rock classification of Dunham (1962) and Embry and Klovan (1971). The section was measured on a bed–by–bed scale, up to a total thickness of 75.4 m, of which 68.9 m correspond to the Derdere Formation; the overlying 6.5 m belong to the Karababa Formation. The number of samples taken of each bed was a function of stratum thickness. For example, rock samples were collected at the basal, middle and top parts of thick beds, whereas only one sample was required if the stratum was very thin. For the interval belonging to the Derdere and Karababa formations, all beds were sampled.

Thin sections have been prepared and stored in the laboratory of the Geological Engineering Department of METU, Ankara. The limestones with rudists are stored in the laboratory of the Geological Engineering Department of DEU, İzmir.

3. Geological setting and stratigraphy

Southeast Turkey is located on the northwestern part of the Arabian Plate and comprises Precambrian, Mesozoic and Cenozoic rocks (Güven et al., 1988; Perinçek et al., 1991; Yılmaz, 1993; Alsharhan and Nairn, 1997; Okay, 2008; Robertson et al., 2016). The marine Cretaceous sequences in southeast Turkey formed along the northern margin of the Arabian Platform, connected to the Mediterranean Neo–Tethys and located on the passive margin of the Arabian Platform (Sungurlu, 1974; Şengör and Yılmaz, 1981; Harris et al., 1984; Powell, 1989; Philip et al., 2000; Stampfli et al., 2001; Kuss et al., 2003; Schulze et al., 2005).

The Cretaceous succession in southeast Turkey is composed of the Mardin (Aptian to Santonian) and Adıyaman (Campanian–upper Maastrichtian) groups (Çoruh et al., 1997; Yılmaz and Duran, 1997) (Fig. 2). The Mardin Group is a widely distributed sequence which is divided into four distinctive formations, from bottom to top: Areban, Sabunsuyu, Derdere and Karababa (Fig. 2), all of which are exposed around the Kilis area (Keskin et al., 1974; Görür et al., 1981; Cros et al., 1999; Gül et al., 2001). The basal transgressive Areban Formation is represented generally by sandstone, sandy limestones and dolomites with interbedded shale which conformably overlie carbonates of the Sabunsuyu Formation (Görür et al., 1981). The Sabunsuyu Formation consists mostly of dolomites and limestones; this, in turn, is overlain conformably by limestones of the Derdere Formation (Çelikdemir et al., 1991). The Derdere Formation comprises organic–rich limestones at the base,

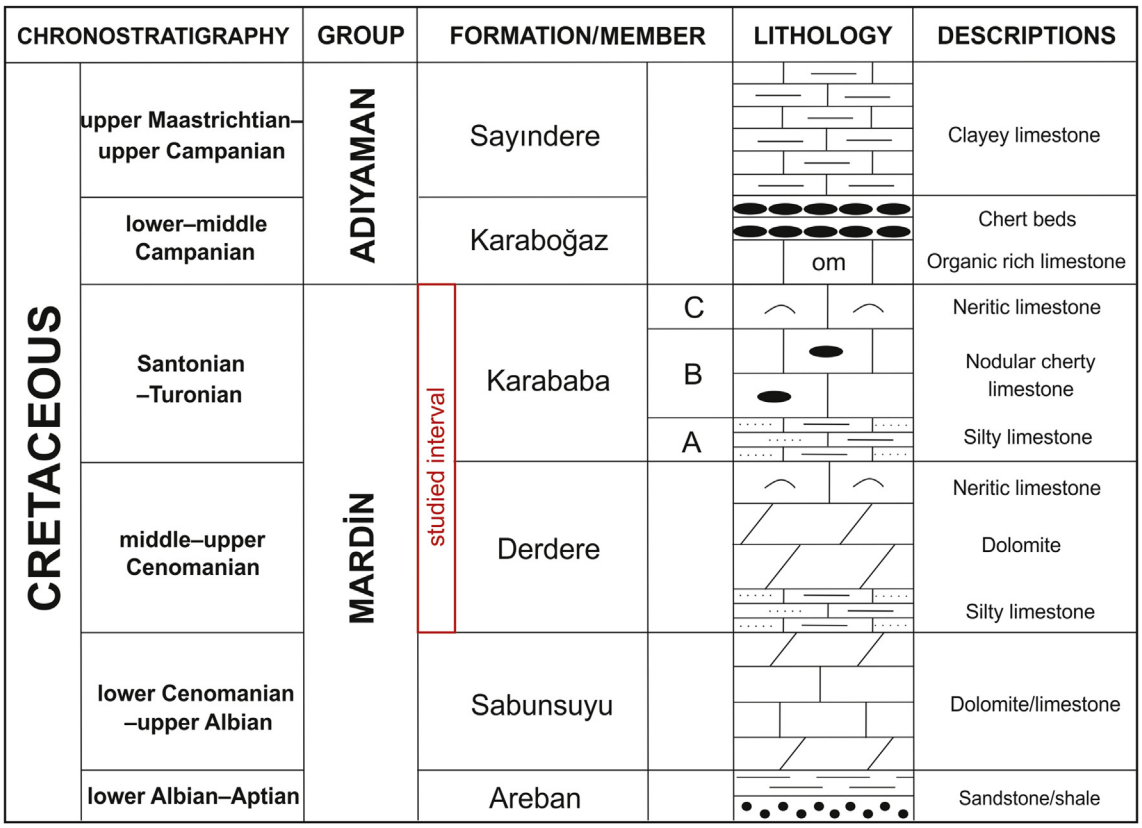

Fig. 2. Columnar section of Cretaceous lithostratigraphical units in the Kilis area (modified from Cros et al., 1999; no vertical scale implied). The red square denotes the interval studied here. (For interpretation of the references to colour in this figure legend, the reader is referred to the Web version of this article.)

dolostones and dolomitic limestones in the middle and skeletal and non–skeletal limestones in the upper part (Mülayim et al., 2019). The Karababa Formation consists of thin– to medium–bedded dark grey, organic–rich/planktonic foraminifera–bearing limestones in the lower part (Karababa–A), medium–thick–bedded nodular cherty limestones in the middle part (Karababa–B) and mainly neritic bioclastic limestone in the upper part (Karababa–C) (Çelikdemir et al., 1991; Görür et al., 1991).

The Derdere Formation is directly overlain by the Karababa Formation in the Sabunsuyu section. The sharp boundary and poor palaeontological indicators in the Turonian may be indicative of a short hiatus between these two formations in the area. Some evidence of hardgrounds was also observed on the surface, such as a pinkish crust and faint bioturbations, but such discordance might be the result of condensation during the time span of the Oceanic Anoxic Event (OAE) reported from the Cenomanian/Turonian boundary in southeast Turkey (Mülayim et al., 2019) and on the Arabian–African platform (Bauer et al., 2001; Abdallah, 2003; Saber et al., 2009; Hajikazemi et al., 2010; Frank et al., 2010; El–Sabbag et al., 2011). Indeed, we have focused on the sedimentological and palaeontological features of the rudist–bearing platform–type carbonates within the Derdere and Karababa formations in the Sabunsuyu stratigraphical section, as presented below:

4. Results

4.1. Biostratigraphy

Bioclasts are dominant components throughout the section and comprise mainly echinoderms (roveacrinids), bivalves and subordinate ostracods, gastropods, bryozoans and annelids. Pithonellids are frequent and occur abundantly in some beds with a minor amount of bioclasts. Rare benthic foraminifera, such as *Meandrospira* sp., *Dorothia* sp., Gavelinellidae and Lenticulinidae are uncommonly associated with pithonellids and planktonic foraminifera. Despite the presence of these bio–fragments and benthic foraminifera throughout the section, they do not help unravel the chronostratigraphy of the succession. Therefore, rudists and planktonic foraminifera seem to be the prime components for determining the age of the formations, as explained below.

Planktonic foraminifera are also rare throughout the succession. These poor assemblages are represented by r–selected taxa, dominated by Hedbergellidae, which are described from the base and the middle/upper part of the Derdere Formation. *Asterohedbergella asterospinosa*, characterised by a tubulospinate extension in the last chamber(s) of the final whorl, has been rarely documented so far, with records from middle to upper Cenomanian strata in Israel (Hamaoui, 1965; Loeblich and Tappan, 1988; BouDagher–Fadel, 2012). The study of rudist facies in southeast Turkish carbonate ramps and their comparison with those of Arabian Plate allow a better determination of the age of the Derdere and Karababa formations. These biostratigraphical data indicate a middle–late Cenomanian and Coniacian–Santonian age for Derdere and Karababa formations, respectively.

4.2. Sabunsuyu section

This section is located to the northwest of the city of Kilis and represents an excellent outcrop of rudist–bearing limestone that allowed us to understand the stratigraphy of the ramp–type carbonate sequence (Derdere and Karababa formations). Our new observations have shown that these formations consist of, in ascending order (Fig. 3).

i) a 4–m–thick, well–bedded, thin– to medium–grained, beige, dark brownish, dolomitic limestone and limestone with shales interbedded in the lowermost part of Derdere Formation; these exhibit also limonitisation (Fig. 4). Exogyrine oysters are abundant in (wavy and parallel) shale layers with calcite veinlets. Abundant small planktonic foraminifera, pithonellids, rare roveacrinids and benthic foraminifera are also present in dolomitic thin limestone beds. Dolomitisation and silicification are common in microfossils. Sedimentary structures such as predominantly parallel lamination, locally wavy and cross lamination and grading are frequent; recognised taxa include *Asterohedbergella asterospinosa*, *Muricohedbergella planispira*, *Globigerinelloides* sp., *Pithonella ovalis*, *Bonetocardiella conoidea*, *Calcisphaerula innominata*, Gavelinellidae, Hedbergellidae indet., many Calcisphaerulidae indet. and Roveacrinidae.

ii) a 19.32–m–thick, thin–bedded intercalation of dark grey, massive dolomitic limestones/dolostones and grey, cherty limestones (nodular and band) with fine lamination, cross–stratification and calcite veinlets in texture. Chert bands are parallel to the strike of the limestones. Bioturbations are rarely observed. Dolomitisation phenomena are diffused in the lower part of the orders (I–II) and can lead to near–complete obliteration of original textures. More frequently, very thin to thin layers are recognisable with different dolomitisation intensity. Many of the bed boundaries correspond to sharp surfaces. These latter are in some cases represented by dolomitised thin layers that may laterally thicken. Roveacrinidae, Hedbergellidae indet. and Calcisphaerulidae indet. have been recognised. The cherty limestones comprise well–preserved planktonic foraminifera such as *Asterohedbergella asterospinosa* (Fig. 5).

iii) a 14.93–m–massive to very thick–bedded intercalation of grey, dolomitic limestones/dolostones and dark grey, unfossiliferous massive limestones. These dolomitic limestones do not yield any index microfossils. Dolomitisation is a common characteristic of this part of the succession; it may characterise beds or alternating millimetre– to centimetre–scale layers. In some cases, it may completely obliterate preceding structures. Dolomitised layers show undulating contacts, locally indented with non–dolomitized lithologies. These phenomena attenuate upwards in the interval.

iv) a 10.55–m–thick, medium–to very thick–bedded, grey, rudist–bearing limestones, bioclastic limestones and limestone intercalations. Two rudist–bearing limestones are distinguished from base to top in this part of the section. The lower one is very thick and consists mainly of radiolitid fragments, of which large quantities are of angular/subangular and poorly sorted nature; however, some transverse and oblique sections of *Durania/Sauvagesia* and *Biradiolites* sp. are rare. Some echinoids with spines are also present. The upper rudist–bearing limestones alternate with limestones and are around 3 m thick. These consist mainly of radiolitid rudists such as *Durania acuticostata* accompanied by *Sauvagesia* cf. *sharpei* and ?*Bournonia* sp. The pectinoid bivalve *Neithea fleuriausiana* has also been observed in these limestones. Roveacrinid skeletons are locally dissociated and found scattered within mud–supported matrix. These rudist–bearing limestones do not yield foraminifera. Bioturbation is occasionally observed in this part of the section. Calcite veinlets are also common in this interval. Benthic foraminifera are characterised by the presence of *Dorothia* sp., *Meandrospira* sp., Gavelinellidae and Lenticulinidae, in the first few tens of meters and in the top of the section. Pithonellids (Calcisphaerulidae indet., *Pithonella ovalis* and *Bonetocardiella conoidea*) and occasional planktonic foraminifera (*Globigerinelloides* sp., Hedbergellidae indet. and *Muricohedbergella planispira*) are associated with the previous species upwards into the succession (Fig. 5).

v) a 1–m–thick, medium–bedded limestone and very thin–bedded limestone, interbedded with chert bands. Planktonic foraminifera and pithonellids are present (*Pithonella ovalis*, Hedbergellidae indet. and Calcisphaerulidae indet.; see Fig. 5).

vi) a 6.5–m–thick upper part, composed of grey, fossiliferous, very thick– to medium–bedded limestones and bioclastic limestones in alternation. The upper part is characterised by grey, massive, very thick rudist–bearing limestones containing mainly rudist shell fragments. Indeterminate radiolitid fragments are abundant; *Sauvagesia* and *Radiolites* have been noted. Caprinids are very rare, only *Caprinula* sp. (*C.* cf. *sharpei*) having been noted. Bivalves, gastropods, echinoid fragments and roveacrinids are abundant in these limestones, but poor preservation precludes specific identification. Peloids are abundant throughout the succession. These limestones can present enriched foraminiferal levels as well as *Asterohedbergella asterospinosa* and *Globigerinelloides* sp. Planktonic foraminifera appear with a higher frequency upwards and are found in alternations of wackestone with benthic foraminifera (Lenticulinidae, *Mendrospira* sp., *Dorothia* sp.) (Fig. 5).

vii) a 5.4–m–thick, very thick–bedded limestone containing two rudist–bearing limestones characterised mainly by abundant ichthyosarcolitids. The first rudist–bearing level is very thick and consists usually of small ichthyosarcolitids. The rudist fauna is monospecific and consists mainly of *Ichthyosarcolites triangularis.* Indeterminate bivalves have also been observed. The second rudist–bearing limestone is very thick and with mainly large *Ichthyosarcolites triangularis* and rare *Ichthyosarcolites monocarinatus.* There are ichthyosarcolitid fragments in the rudist–bearing limestones, but they are accumulated in their original environment and are not reworked and transported. Peloids are abundant throughout the succession. Benthic foraminifera (Gavelinellidae) (Fig. 5), molluscs and roveacrinids are also present. A hardground–type surface is seen at the top of this interval.

viii) a 3–m–thick part of the succession consists of dark grey, thin–bedded silty limestones. Some pithonellids with glauconite grains and *Pithonella ovalis*, *Bonetocardiella conoidea*, Heterohelicidae, *Hedbergella* indet. and Calcisphaerulidae indet. can be described (Fig. 5).

ix) a 3.5–m–thick, grey, thick–bedded limestone consisting of two rudist–bearing limestone levels. Dolomitisation and bioturbation are usually observed. Upwards in the section, intercalations of grey limestones and bioclastic limestones with rudists are seen. The thickness of the rudist–bearing limestones is laterally variable from thick to very thick. The lower rudist–bearing limestones contain small numbers of *Bournonia excavata*, *Apricardia* sp. and indeterminate requieniids. Other bivalves are represented by abundant, but unidentifiable specimens. Rudists are usually in life position; however, intense fragmentation and accumulation of rudists and bivalves can be observed. In other cases, they are associated with very thin bioclastic laminae which locally show thin accumulations of rudist shells, both pristinely preserved and highly abraded. The bioclastic matrix (packstone) is composed almost exclusively of bioeroded rudist–shell fragments, associated with rare benthic foraminifera (*Dorothia* sp.) (Fig. 5). Molluscs, echinoid fragments and roveacrinids are also present. Peloids are rare throughout the succession. The upper rudist–bearing limestone consists mainly of *Bournonia excavata* in growth position, and also including fragments. Fragmentation of rudists is rarer than in the lower rudist–bearing level.

4.3. Rudist facies and age

Rudists have been described from the Derdere and Karababa formations (Figs 6–8). Radiolitid fragments are present in the

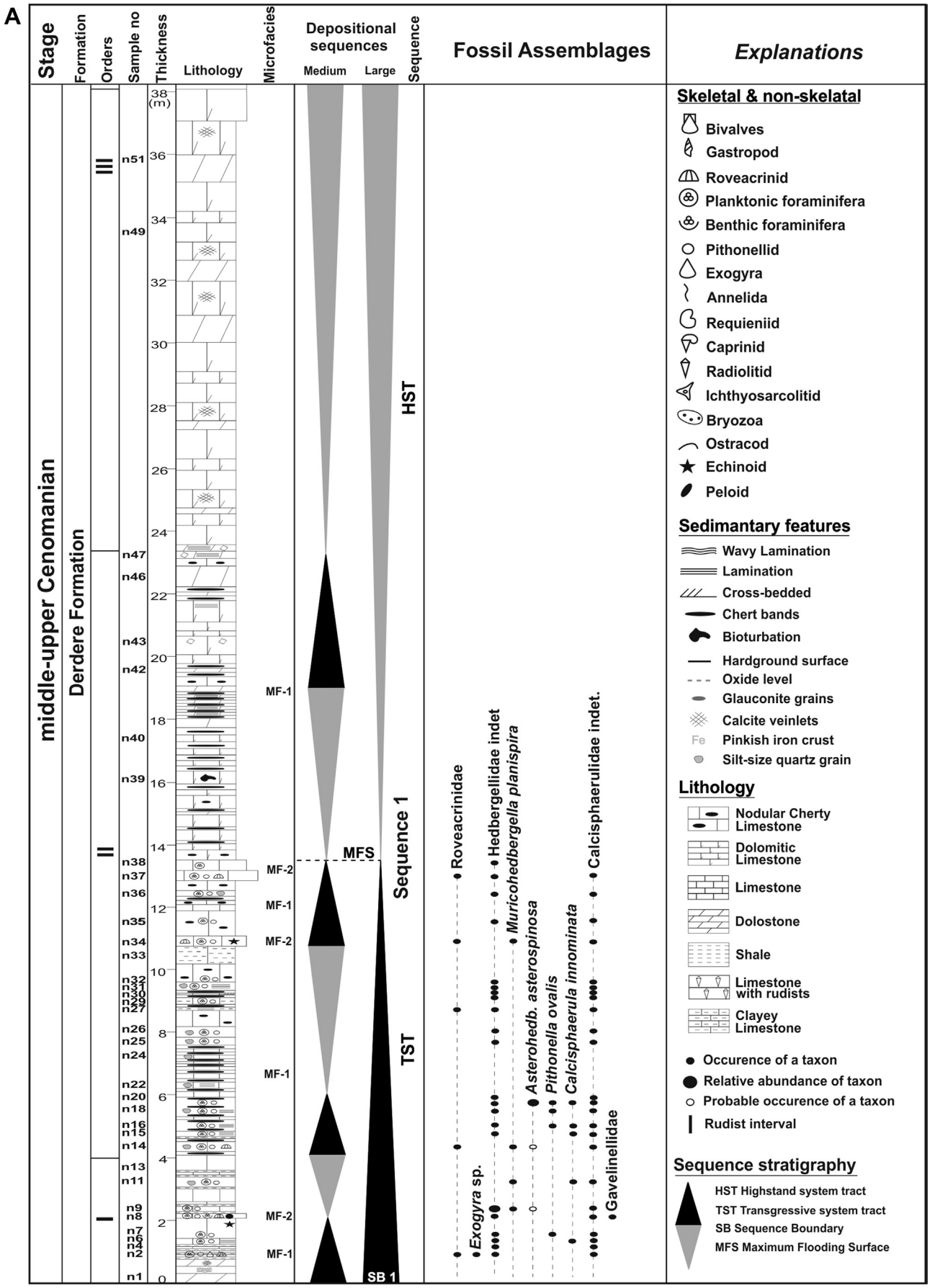

Fig. 3. A, B. Distribution of rudists, foraminifera and other organisms and changes in composition and sequence–stratigraphical framework for the Derdere and Karababa formations in the Sabunsuyu section (southeast Turkey).

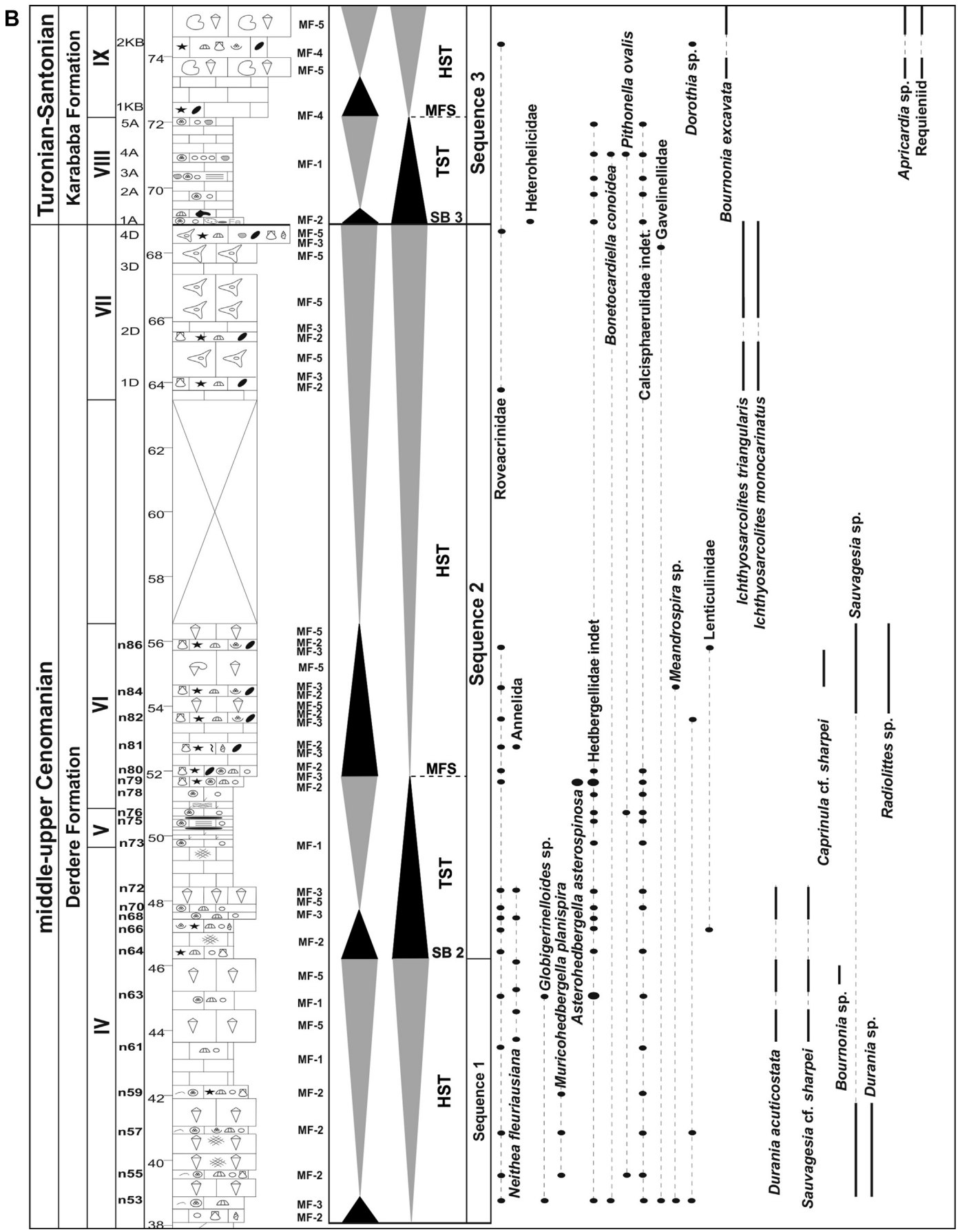

Fig. 3. (*continued*).

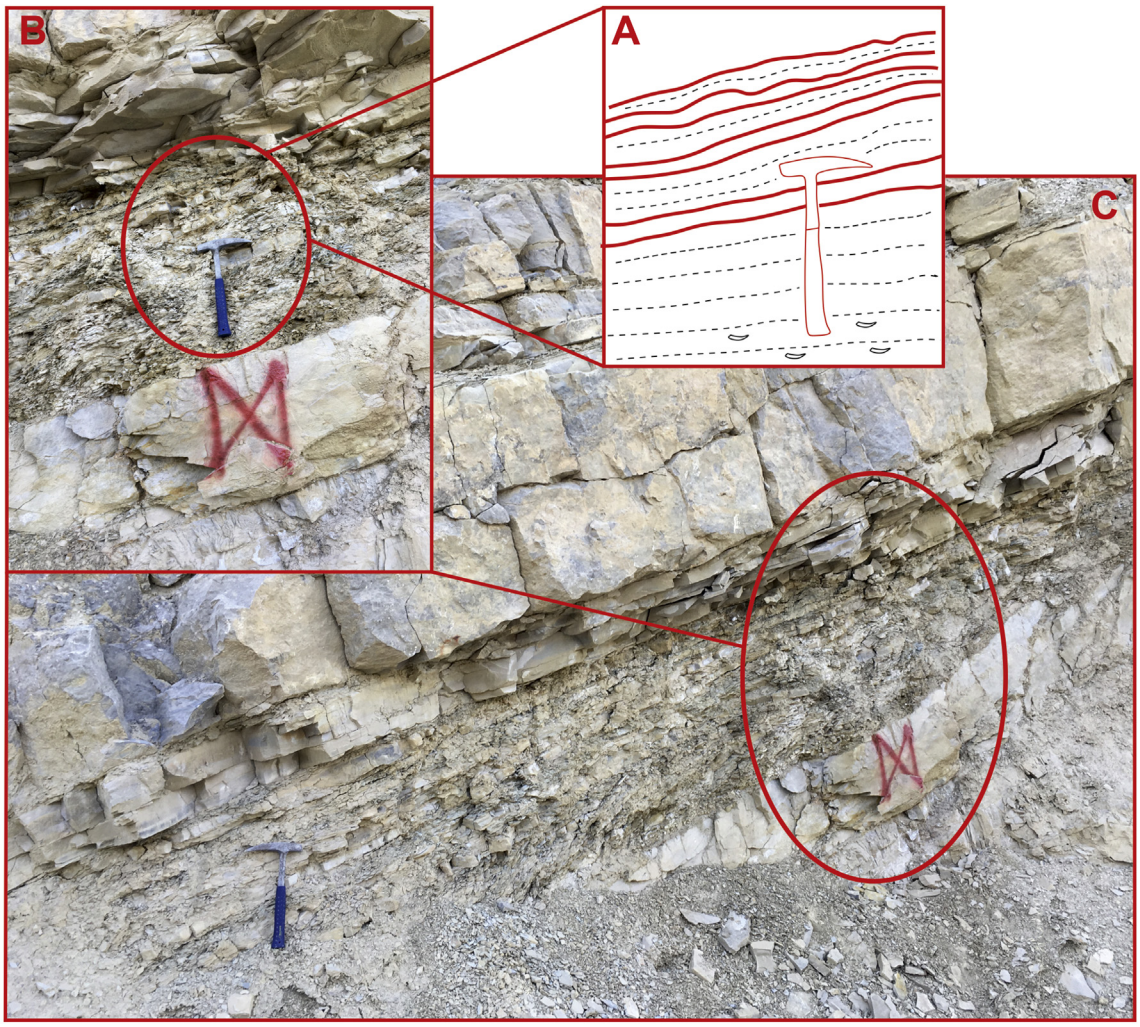

Fig. 4. Outcrop evidence of (1st order) intercalation of dolomitic limestone and shale beds at the base of the Derdere Formation. Exogyrine oysters are observed in shale layers, which are indicated in the area (red square, a), just below the hammer. (For interpretation of the references to colour in this figure legend, the reader is referred to the Web version of this article.)

middle part of the Derdere Formation. Some subsquare right valve sections with more and less developed ribs and circular to semi–circular sections might belong to *Biradiolites* sp. and *Durania* sp., respectively (Fig. 6B–D). However, some radiolitids of biostratigraphical importance in the upper Cenomanian, such as *Durania acuticostata* and *Sauvagesia* cf. *sharpei*, are found around the middle part of the formation. Many transverse sections of right valves of *D. acuticostata* show characteristic features such as a thin outer shell layer, strong and acute ribs delimited by wider sinuses, wide and flat ventral and slightly concave posterior radial bands separated by a concave interband (Fig. 6F–H). This species is well known from the upper Cenomanian of Friuli, Italy (Caffau et al., 1996) and Trieste, Italy (Pons et al., 2011). Some conical right valves in growth position and transverse sections of *S. sharpei* present finely ribbed ornamentation, the flat and slightly protruding radial structures separated by a concave interband and a very small, triangular ligamental ridge (Figs 6J, 7A, B). The age of *S. sharpei* is late Cenomanian at its type locality (Alcantara, Portugal); the species is well known from the upper Cenomanian or undefine Cenomanian of the northern and southern sides of the Mediterranean Tethys (Steuber, 2002; Chikhi–Aouimeur, 2010; Pons et al., 2011), but it has been also recorded from the Turonian in some studies. It has recently been described for the Arabian Platform from the upper Cenomanian of northern Jordan by Özer and Ahmad (2015, 2016). *Neithea fleuriausiana* co–occurs (Fig. 6I, J). Although this species ranges from the Cenomanian to the Turonian in Tethyan rudist limestone (Dhondt, 1973), it was found together *D. acuticostata* and *S. sharpei* in upper Cenomanian limestones of Friuli, Italy (Caffau et al., 1996). Thus, faunal content shows clear similarities between these localities.

Some small oval sections of radiolitids seem to show the radial structures of *Bournonia* in these levels of the middle part of the section (Fig. 7D). These may be correlated even with those of *B. africana*, as demonstrated by Steuber (1999, text–fig. 29 F). However, to date this genus has not been recorded from the Cenomanian, which we list it here with a query. The bioclastic limestones of the uppermost middle part of the section contain poorly preserved canaliculate rudist fragments. Some of the transverse sections of the right valve are suboval, showing only a very thin internal shell layer consisting of one or two rows of small rounded pallial canals in the posterior part (Fig. 7F). The poor canaliculation is characteristic of *Caprinula sharpei*, differing from other species of the genus, as demonstrated by Douvillé (1888) and Özer and Ahmad (2016). *Caprinula sharpei* is suggestive of a Cenomanian age in the central part of the northern side of the Mediterranean Tethys (Steuber, 2002). The species is known from the Arabian Platform from the upper Cenomanian of northern Jordan (Özer and Ahmad, 2016) and has recently been noted from the Central

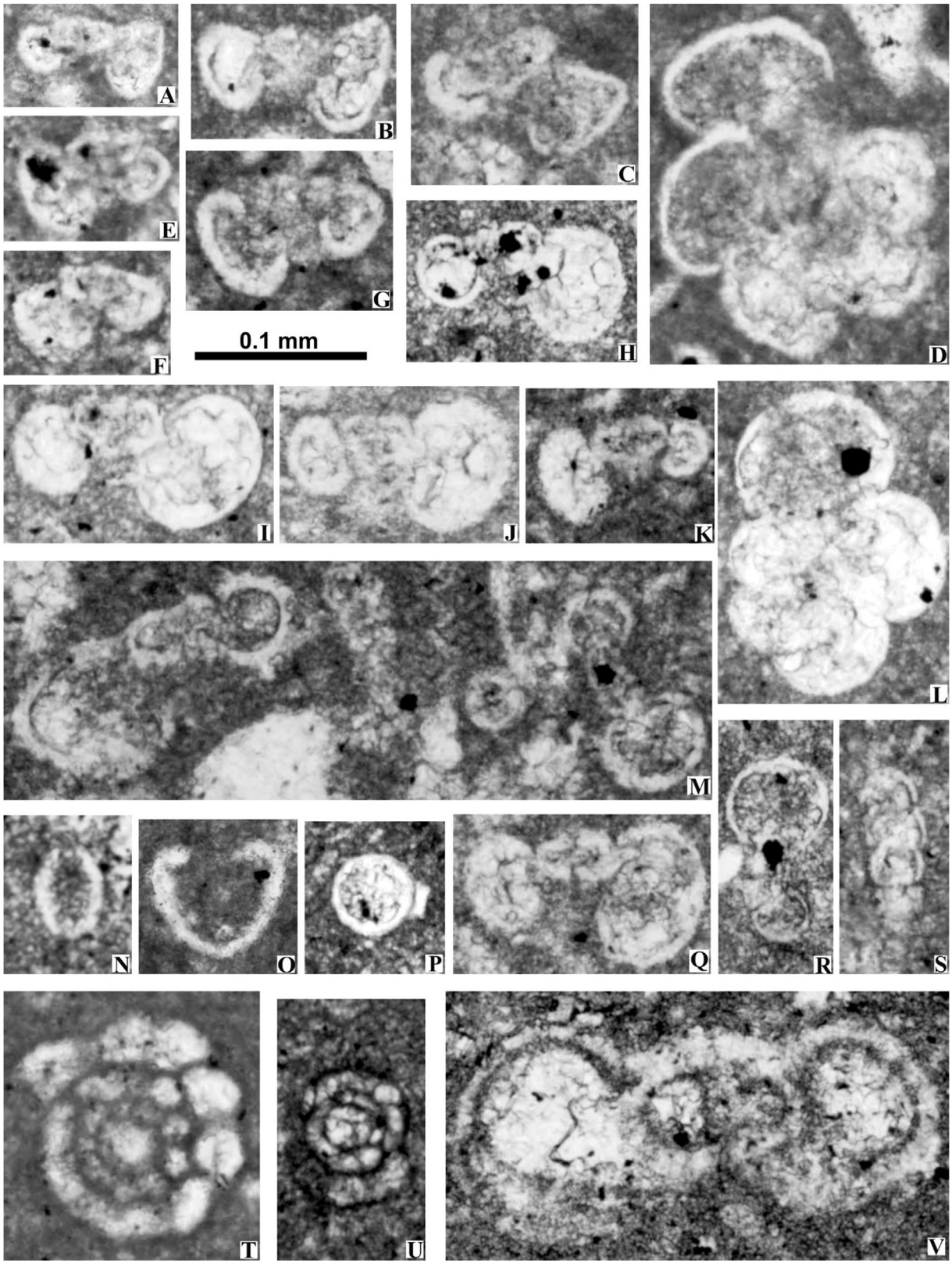

Fig. 5. Planktonic foraminifera. A–C. *Asterohedbergella asterospinosa*, MU, samples 19, 79 and 79, respectively; D–L. Hedbergellidae indet., MU, samples 79, 1D, 1A, 1D, 19, 19, 79, 63 and 63, respectively; M. Hedbergellidae indet. (left) and *Globigerinelloides* sp. (right), MU, sample 86; Q. Hedbergellidae indet., MU, sample 80; R. *Globigerinelloides* sp., MU, sample 63; S. Heterohelicidae indet., MU, sample 1A; pithonellids: N. *Pithonella ovalis*, MU, sample 7; O. *Bonetocardiella conoidea*, MU, sample 53; P: *Calcisphaerula innominata*, MU, sample 19; benthic foraminifera: T, U. *Meandrospira* sp., MU, samples 53 and 84, respectively; V. Gavelinellidae, MU, sample 8. Abbreviation: MU – Mersin University.

Taurides (Turkey), in the lower–middle Cenomanian by Özer and Kahrıman (2019). The radiolitid sections belong to *Biradiolites* sp. and may be *Radiolites* is also found in these bioclastic limestones (Fig. 7G).

The upper part of the Derdere Formation comprises mainly monospecific ichthyosarcolitids, *Ichthyosarcolites monocarinatus* and *I. triangularis* (Fig. 8A–I). The former species presents abundant right valve sections showing typical characteristics of the species such as a slightly elliptical transverse section of the right valve and a single flange on the antero–ventral side (Fig. 8B–F). The external shell layer is partially observed, the internal shell layer consists of dense, ovaloid and round pallial canals, a single very thin tabula; elongated teeth sockets of the left valve are observed. Some curved left valves are present. These sections present close similarities to descriptions of Slišković (1966), Polšak (1967), Cestari et al. (1998), Pleničar and Jurkovšek (2000), Troya Garcia (2015), Rineau and Villier (2018) and Özer and Kahrıman (2019). *Ichthyosarcolites triangularis* has a triangular shell shape with a single projecting flange on the dorsal side of the right valve, a thick internal shell layer with dense, small, round to ovoid pallial canal sections and many concave tabulae in the internal moulds of the body cavity (Fig. 8G–I), which are characteristics of the species (Desmarest, 1817; d'Orbigny, d1847, 1850; Troya Garcia, 2015; Rineau and Villier, 2018; Özer and Kahrıman, 2019). Ichthyosarcolitids suggest a Cenomanian date, having been described from lower, middle–upper and upper Cenomanian formations in the periphery of the Mediterranean Tethys (Steuber, 2002). They have recently been described from the Central Taurides (Turkey) from the lower–middle Cenomanian by Özer and Kahrıman (2019). The find of this species in the uppermost part of the formation suggests a late Cenomanian age.

The rudist fauna of the Karababa Formation is characterised by an abundance of *Bournonia excavata*, but *Apricardia* sp. and indeterminate requieniids are also present (Fig. 8J–O). *Bournonia excavata* represents small, cylindro–conical right valves, with subrounded dorsal side, the ventral radial band being more developed than the posterior one and the concave interband separating the radial bands (Fig. 8K–M). *Apricardia* sp. shows a small, strongly coiled left valve and a conical, slightly capuloid right valve (Fig. 8N, O). The age of *B. excavata* is early Santonian at its type locality (d'Orbigny, 1850; Toucas, 1907; Macé–Bordy, 2007). However, it has been recorded from Coniacian levels in Germany and Spain and Santonian strata in Italy, France, Spain and Romania (Steuber, 2002; Cestari, 2008; Lucena Santiago, 2014). In previous studies (covering Italy, Bosnia–Herzegovina, Croatia, Cuba, Afghanistan and Somalia), also a Campanian–Maastrichtian date has been attributed to *B. excavata*, but the majority of these lack figure(s) and descriptions from (for references, see Steuber, 2002). Some studies present merely figure(s) and/or descriptions of this species from the Campanian–Maastrichtian or Maastrichtian of Montenegro, Italy, Guatemala and Iran (see Steuber, 2002; Khazaei et al., 2010). Thus, a Campanian–Maastrichtian date for *B. excavata* is questionable (Steuber, 2002; Lucena Santiago, 2014), but the discussion continues. In the present study, we favour dating *B. excavata* as Coniacian–Santonian, with respect to its stratigraphical distribution in Tethyan areas and the age of the Karababa Formation.

4.4. Rudist interpretation

Rudists constitute exclusive bioclasts, characterised mainly by radiolitid species in the middle part of the Derdere Formation. Most of the calcitic outer shell layer of bioclasts is completely recrystallised and commonly unbroken. The cellular prismatic structure of this layer can be partly observed in some fragments. The aragonitic inner shell layer of radiolitids is unprotected due to dissolution. In some cases, the shells are disoriented and assume multiple superimposed orientations in the same layer. Isolated individuals are also common; small bouquets are rare. Bioerosion may have led to the formation of elongated fragments found both in bioclastic fractions, together with large fragments, where they appear oriented. It appears in this section that rudists are associated with bioclastic levels composed almost exclusively of comminuted rudist shells, lodged even in between close–set individuals. The bioclasts derive from rudist, bivalve and roveacrinid shells and appear to be bioeroded and moderately abraded. They laterally interfinger with small–bioclastic to large–scale limestone beds in which the bioclasts consist of poorly sorted, bioeroded and fairly abraded rudist, bivalve and echinoid shell fragments in a silty–bioclastic wackestone matrix. In some cases, grading appears well developed, suggesting that the final deposition of skeletal elements was caused by high–energy events such as storm flows. A small number of holes in the bioclasts were observed in field studies and also in studies of thin section. These are very rare and small, probably bored by algae and fungi. Physical breakdown seems to be the main piece of evidence of bioerosion.

In the Derdere Formation, sheet–like and tabular bodies are usually associated with monospecific rudist associations at the top of the unit. These do not exhibit horizontal orientation. The rudist shells, in upright growth position, appear either clustered or as isolated individuals. The top of this tabular body may be associated with an incipient hardground. Bedding is often evidenced by such surfaces which are observed especially at the Cenomanian–Turonian boundary. This type of shell accumulation characterises the top bed of the Derdere Formation (upper Cenomanian). Grain sorting is poor and bioclasts are bioeroded and moderately abraded; shells are packed. However, rudist–rich levels appear to be concentrated in the upper two metres, whereas they become rare upsection; rudists often form levels. In other cases, they appear as oriented, dispersed, toppled individuals of pristine preservation or slightly reworked. The upper shell bed is associated with a sharp basal contact with the Karababa Formation. Most of the rudist shell beds in the Derdere Formation are composed of large numbers of shells that are oriented parallel to subparallel with respect to bedding. These beds have a discontinuous shell distribution laterally. The broadly spaced, imbricated stacking of the radiolitid shells implies originally loosely clustered shells. Storm waves may have been caused by toppling and dense stacking of shells.

In the Karababa Formation, shell beds are horizontal, in lateral view orientation. Most shells show signs of bioerosion; they are highly abraded, while some of them are still articulated. Shell fragments dominate over complete shells; fragmentation and abrasion are abundant and shells are comminuted beyond taxonomic recognition. Their orientation is random, while species diversity is low. These monospecific shell beds are thick. Rudists in growth position are rare; most of them appear to have toppled and locally oriented, but may have been reworked. Rudist–rich beds are frequent in the uppermost part of the series, whereas they become rarer in the middle but are abundant and thicker in the middle–upper part of the Karababa Formation. Good shell preservation is indicative of a more energetic environment but the presence of unbroken shells suggests that water circulation was not so effective in destroying shells. Differences in shell orientation recognised at some levels suggest variations in current direction. Species diversity is low. The removal of finer matrix produced by bioerosion and *in–situ* reworkings of skeletal elements, rather than transport, are linked to periods of prolonged exposure and low sedimentation rates.

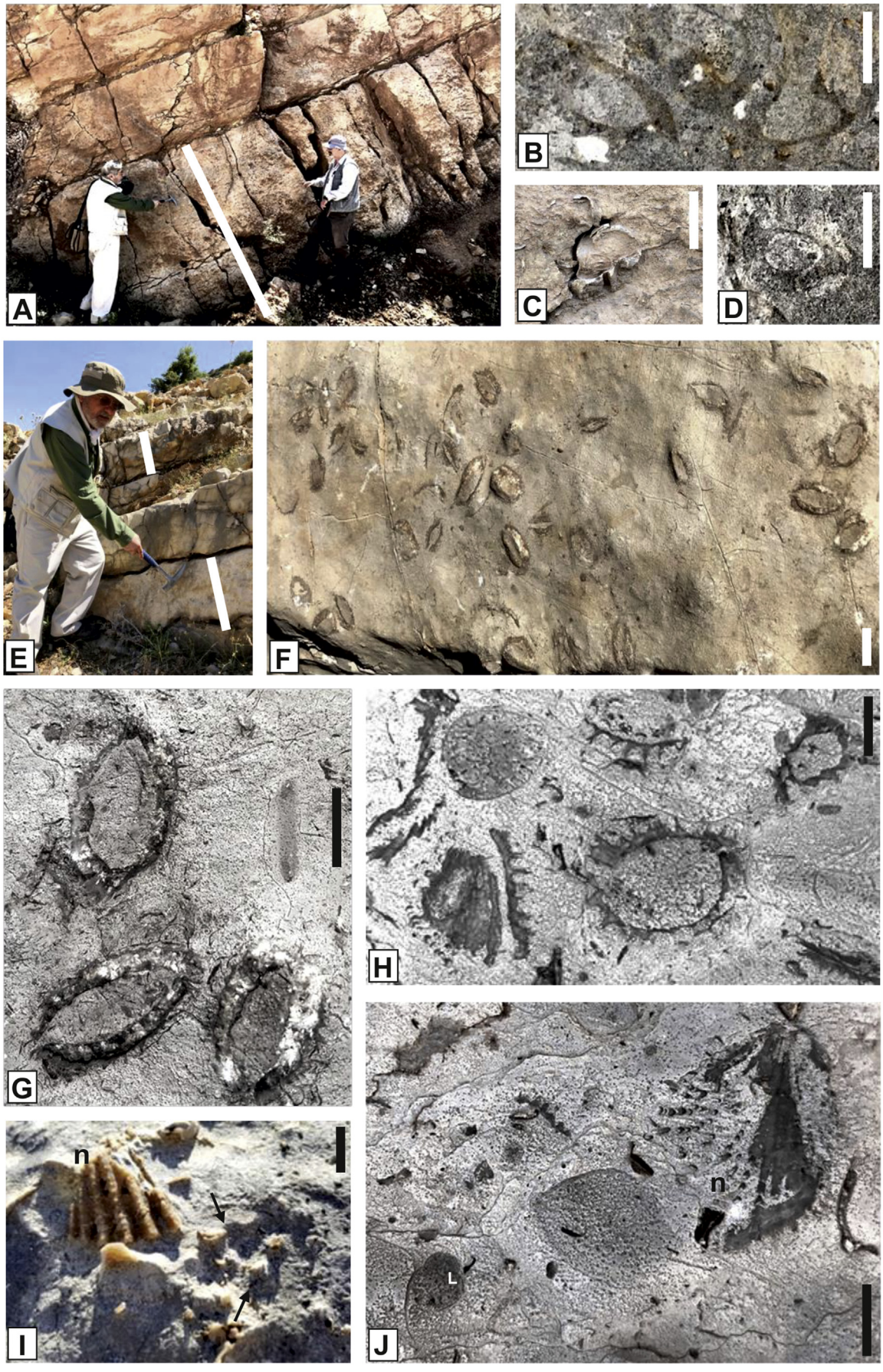
A
B
C
D
E
F
G
H
n
I
n
L
J

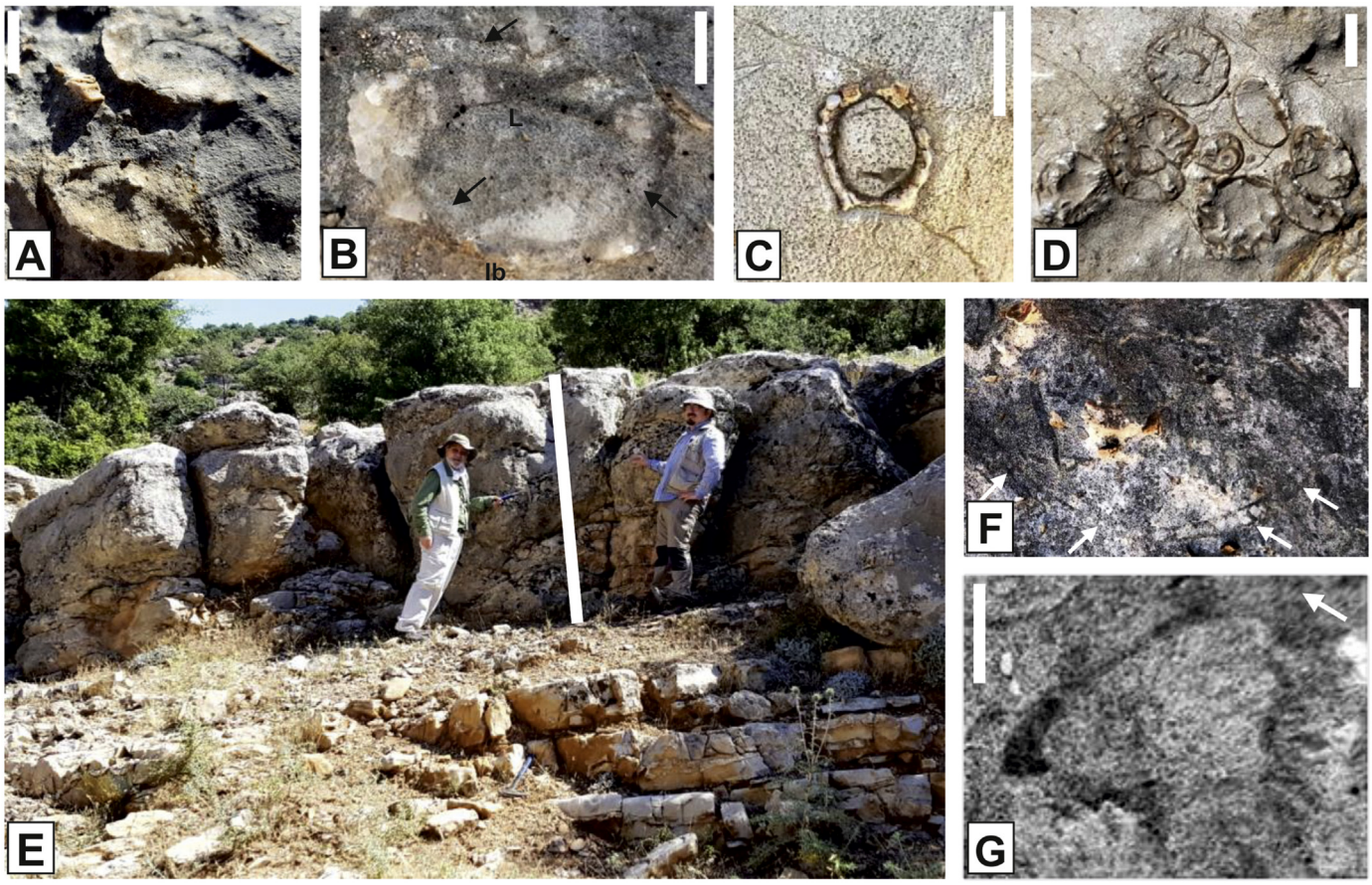

Fig. 7. Rudist–bearing limestones of the Derdere Formation, outcrop photographs. A. *Sauvagesia sharpei*, two right valves in growth position. B. *Sauvagesia sharpei*, transverse section of right valve showing thick outer shell layer, short triangular ligamental ridge (L), flat and slightly protruding radial structures separated by a concave interband (Ib). Cellular structure seems to be partially preserved (thin black arrows). C. *Bournonia*? sp., transverse section of right valve; radial structures showing some similarities to those of the genus. D. Stalk elements of crinoids. E. Field views of rudist–bearing limestones of unit VI (scale bar equals 2 m). F–G. Closeup of previous photograph. F. Poorly preserved transverse section of right valve of a canaliculated rudist fragment showing very thin internal shell layer with one or two rows of small rounded pallial canals in posterior part (white arrows), as in *Caprinula sharpei*. G. *Biradiolites* sp., transverse section of right valve showing acute ribs (scale bar equals 10 mm in all photographs, except E). (For interpretation of the references to colour in this figure legend, the reader is referred to the Web version of this article.)

4.5. Taphonomic aspects

In the Sabunsuyu succession, rudists represent a greater proportion of fossil assemblages from Cenomanian– Santonian limestones. Taphonomic observations yield many data on the sedimentary processes in operation. Rudists occurred in three palaeoecological morphotypes, i.e., elevators, clingers and recumbents (Gili et al., 1995; Skelton and Gili, 2002) and their palaeoecological characters have recently been reviewed by Gili and Götz (2018). It seems that rudists were rarely fossilised in life position because of storms that could cause toppling of shells. However, the conical and cylindro–conical upright position of elevator radiolitids observed may indicate growth position. In a few cases, the small cylindro–conical radiolitid shells show an upward curvature. The recumbent ichthyosarcolitids (Skelton and Gili, 2002; Gili and Götz, 2018) were not observed in any life position. The body cavities of rudists are usually infilled by the surrounding finer bioclastic sediments and/or more commonly by peloids.

5. Microfacies analysis

The microfacies document a mudstone–packstone texture with predominantly rudists, pithonellids, planktonic and benthic foraminifera, echinoids, bivalves and roveacrinid crinoids (Fig. 9). Based on petrographic analysis of the Derdere and Karababa formations, five microfacies are here interpreted to represent inner– to outer–ramp settings.

5.1. Mf–1: laminated/non–laminated, silt–bearing limy mudstone

This microfacies consists of finely textured, dense, dark grey microcrystalline calcite and contains planktonic foraminifera and pithonellids floating in a mud–supported fabric (Fig. 9A). Some parts are thinly laminated in silt–sized quartz (Fig. 9B). Pithonellids are the predominant skeletal grains in this microfacies, ranging from 80 to 90 per cent in abundance and show a concentric wall structure. Roveacrinids range from 1 to 3 per cent in abundance. Fine bioclastic grains are evenly distributed in a micritic matrix.

Fig. 6. Rudist–bearing limestones of the Derdere Formation. A. Field view showing thickness (white bar equals 2.90 m) of lower rudist–bearing limestones of unit IV. B–D. Closeup of previous photograph showing transverse and oblique sections of rudist fragments (B–C. *Biradiolites* sp.; D. *Durania* sp.), scale bar equals 10 mm. E–J. Field views of upper rudist–bearing limestones of unit IV. E. Rudist–bearing limestones alternating with limestones (white bar equals 40–50 cm, indicating rudist–bearing limestones. F–H. Closeup of previous photograph showing transverse sections of monospecific *Durania acuticostata*. Note thin outer shell layer and strong and acute ribs limited by wider sinuses (scale bar equals 10 mm). I. *Neithea fleuriausiana* (n) and small radiolitidis (thin black arrows) in life position (scale bar equals 10 mm). J. Transverse sections of right valves of *Sauvagesia sharpei* (thin black arrows). Note thick outer shell layer, small, triangular ligamental ridge (L) and presence of *Neithea fleuriausiana* (n) (scale bar equals 10 mm). (For interpretation of the references to colour in this figure legend, the reader is referred to the Web version of this article.)

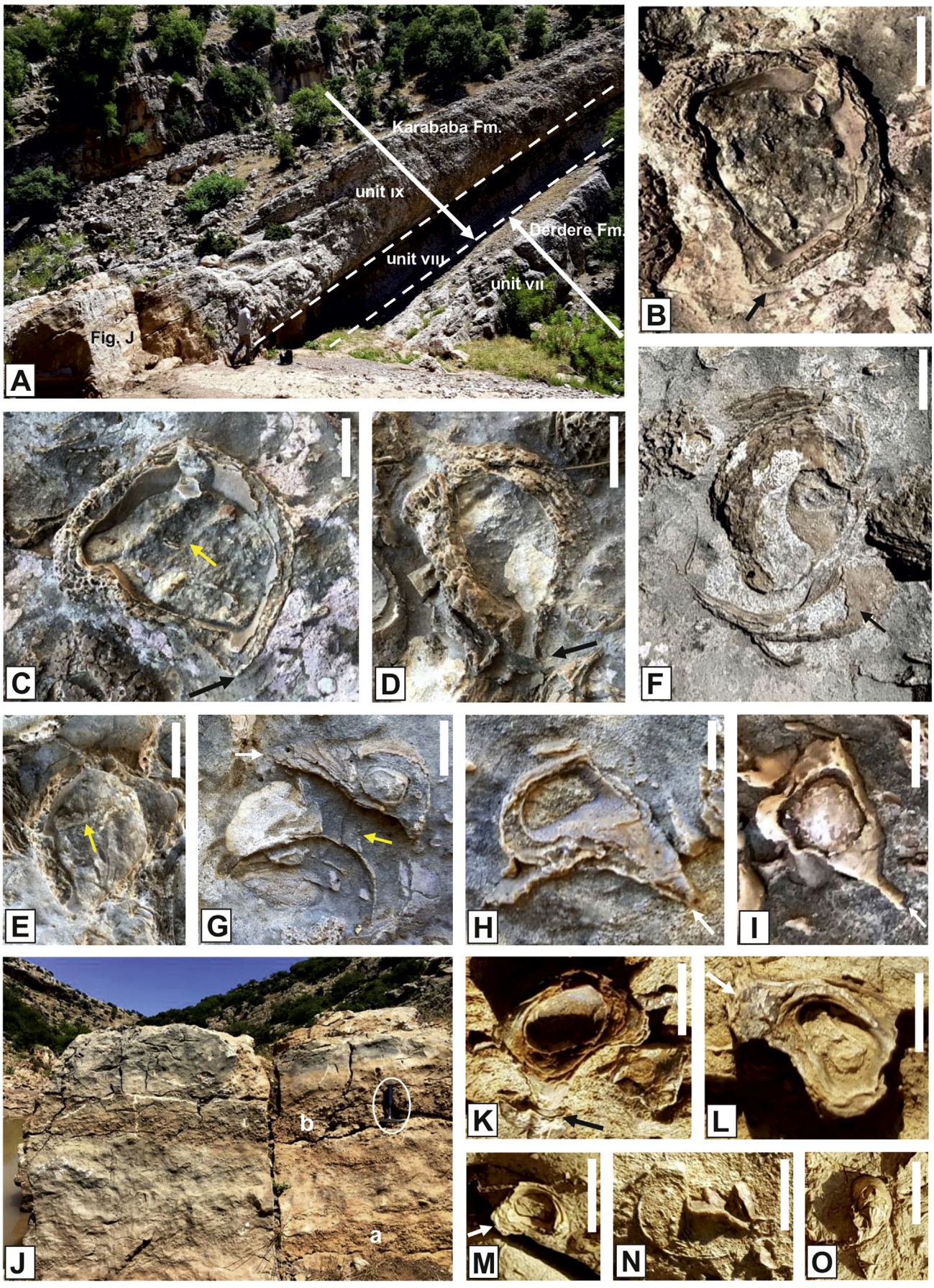
Karababa Fm.
unit IX
unit VIII
unit VII
Derdere Fm.
Fig. J
A
B
C
D
F
E
G
H
I
J
b
a
K
L
M
N
O

Subordinate grains predominantly are roveacrinid bioclasts. Also, the mud shows a slight degree of recrystallisation into xenotopic microspar and is dolomitised in parts. Dolomitisation and silicification are common in microfossils that are poorly preserved. Chambers of some planktonic foraminifera are almost completely replaced by dolomite in places. Dolomite occurs as rhombic crystals or patches which replace the chambers partially or completely in a matrix.

5.2. Mf–2: bioclastic peloidal wackestone/packstone

The main characteristic of this microfacies is the poorly sorting of bioclasts of various sizes which comprise coarse and fine rudist debris, bivalves, roveacrinids, echinoids, as well as planktonic and benthic foraminifera, subordinate ostracods, gastropods, bryozoans and annelids (Fig. 9C). These are distributed in a mud–supported matrix or/and replaced partially to completely by sparry calcite or dolomite. Intraskeletal pores are commonly filled with sparry calcite. Peloidal grains are common constitutes in the packstone texture. Peloids are spherical, ellipsoidal or angular but are mostly well rounded and show weak to moderate sorting. Peloids often merge into a pseudo–micritic matrix, causing a clotted texture. Sparry calcite partly replaces the micritic matrix.

5.3. Mf–3: bivalve and roveacrinid floatstone

This microfacies is characterised by an accumulation of up to >2–mm–sized bivalves and roveacrinids (Fig. 9D, E), embedded in a micritic matrix which is mostly randomly or less commonly concordantly oriented. They are well preserved, positioned obliquely or parallel to bedding and do not show any micritisation. Sparitic shelters and geopetal textures are present. Microcrystalline spar is observed at the top of some valves. Planktonic foraminifera and pithonellids are minor grains.

5.4. Mf–4: echinoderm bioclastic packstone

This microfacies consists of packstones containing mainly echinoid bioclasts (Fig. 9F). and subordinate bivalve and rudist shells. Gastropod, planktonic foraminifera and roveacrinid fragments also occur sporadically. The packstone–depositional texture shows an internal part of a rudist valve filled with calcite cement and intense recrystallisation. Micritic peloids are also common. The allochems are moderately to poorly sorted and account for variable amounts (up to 20 per cent of rock volume). Scarce glauconite pellets are locally observed. Carbonate particles are tightly packed and the micritic/microsparitic matrix is rarely presented.

5.5. Mf–5: rudist floatstone/rudstone

Rudist floatstone/rudstone is characterised by radiolitids and ichthoyosarcolitids (Fig. 9G–H). The silty matrix is composed of fine packstone to wackestone with abundant peloids, skeletal fragments of bivalves, echinoids, gastropods and small benthic foraminifera with a large proportion derived from bioerosion of rudist shells and broken down to silt–sized grains. Finely dispersed dolomite rhombs occur in the matrix locally.

6. Depositional setting

The lithological, biotic and microfacies data obtained document depositional settings in the Sabunsuyu section (Fig. 10) in which rudists partly flourished, were fragmented or reworked through the Cenomanian–Santonian time interval.

6.1. Lithologies and depositional processes

The most prominent rocks in the stratigraphical interval studied are characterised by rudist–dominated, fine– to coarse–grained lithologies, which are made up of intense fragmentation of bioeroded molluscan shells. Hermatypic corals and green algae disappear almost completely at this level. Non–skeletal grains (predominantly peloids) are common. Planktonic foraminifera is generally rare throughout the section, but abundantly present at some levels. The matrix is fine– to coarse–grained and ranges from wackestone to floatstone with a wide range of skeletal particles. These sediments were produced *in situ* on the ramp on which rudist bivalves were the primary sediment producers. The rudist–bearing limestones formed under slightly, moderately and strongly agitated water conditions. The presence of limestones with identifiable rudists, bivalves and roveacrinids, alternating with bioclastic limestones including intensely fragmented faunas of rudists, bivalves and gastropods, document occasional changes in energy conditions on the carbonate ramp, triggered by storm activity. Rudists and other bivalves were actively moved by currents, waves and storms, causing fragmentation and transportation, albeit not far from their original environment. The presence of some limestones with planktonic foraminifera illustrates the effects of occasional open–marine connections within the proximal parts of the outer–ramp.

The middle–upper Cenomanian rudist–bearing limestone sequence of the Sabunsuyu section presents close similarities in terms of features such as alternation and changes of depositional conditions with those of the central Apennines (Carbone et al., 1971) and may also be correlated with the central and eastern regions of the northern Mediterranean Province (Philip, 1980; Özer, 1988; Philip and Mermigis, 1989; Carbone, 1993; Sartorio et al., 1992; Cestari and Sartorio, 1995; Laviano et al., 1998a, b; Steuber, 1999; Di Stefano and Ruberti, 2000; Stössel and Bernoulli, 2000; Korbar et al., 2001; Sarı, 2006a, b; Parente et al., 2007; Sarı and Özer, 2009; Sarı et al., 2009; Cestari and Laviano, 2012; Troya et al., 2011; Frija et al., 2015) and the Gulf of Mexico (Scott, 1990). However, high–energy platform margin depositional environments have been proposed in those studies, rather than the carbonate ramp depositional conditions presented here.

There are lithological similarities of the Sabunsuyu section with those described in previous studies, reported mainly by TPAO in southeast Turkey (see Keskin et al., 1974; Görür et al., 1981; Cros et al., 1999; Gül et al., 2001), but fossil contents of the Derdere and Karababa formations included essentially planktonic

Fig. 8. A. Field view showing rudist–bearing limestones of Derdere (unit VII) and Karababa (units VIII and IX) formations. B–I. Rudists of the Derdere Formation, outcrop photographs (scale bar equals 10 mm). B–F. *Ichthyosarcolites monocarinatus*. B–E. Transverse sections of right valve with single flange on antero–ventral side (black arrow), internal shell layer consisting of dense, ovaloid and round pallial canals, a single very thin tabula (yellow arrow) and elongated teeth sockets of left valve. F. Curved left valve (umbo to right) showing pallial canals in eroded part, some parts may be belong to right valve (black arrow). G–I. *Ichthyosarcolites triangularis*, triangular transverse sections of right valve with single projecting flange on dorsal side (white arrow). Teeth sockets of left valve may be present in part. Concave tabulae observed in internal moulds of body cavity (yellow arrow, in G). J. Field view showing thickness of lower (a) and upper (b) rudist–bearing limestones of unit IX (hammer for scale). K–O. Rudists of the Karababa Formation, outcrop photographs (scale bar equals 10 mm). K–M. *Bournonia excavata*, transverse sections of small right valves showing subrounded dorsal side, ventral radial band (black and white arrows) better developed than posterior one and concave interband. N–O. *Apricardia* sp., small valves, strongly coiled left valve and conical, slightly capuloid right valve. (For interpretation of the references to colour in this figure legend, the reader is referred to the Web version of this article.)

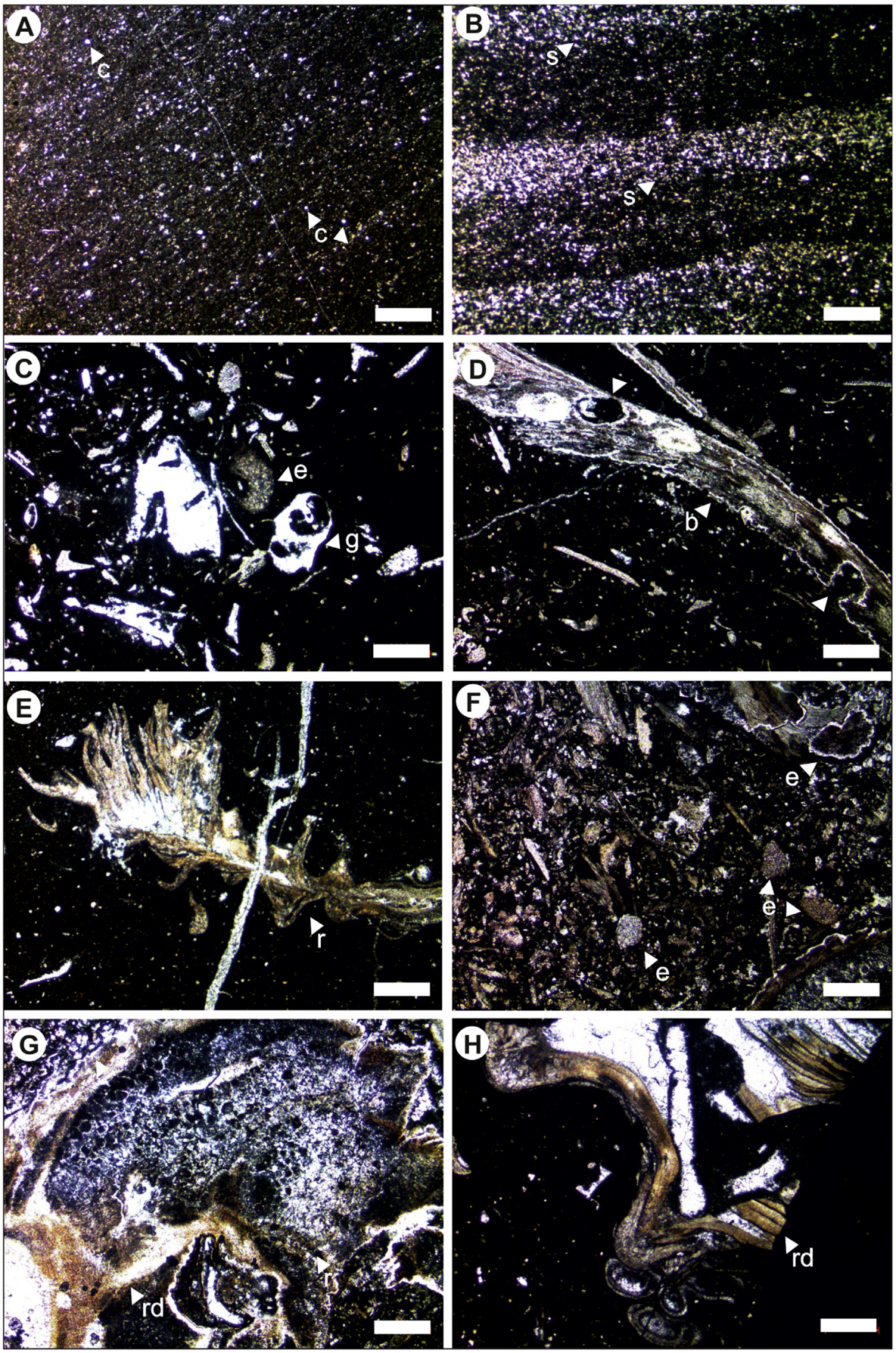
A
c
c
B
s
s
C
e
g
D
b
E
r
F
e
e
e
G
r
rd
H
rd

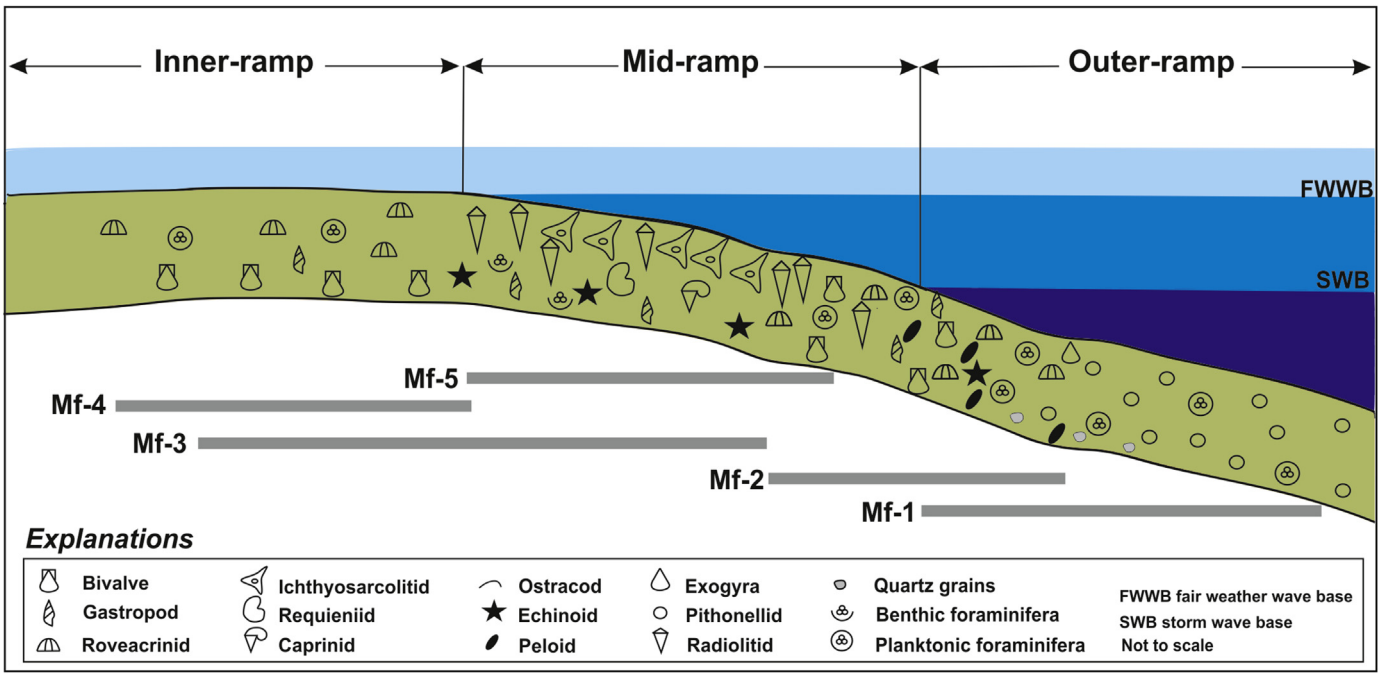

Fig. 10. Depositional model showing microfacies distribution and faunal components for the Cenomanian–Santonian succession in the Sabunsuyu section. The rudist lithosome is the main element of the homoclinal carbonate ramp that thrived in the mid–ramp setting and passed laterally into a deep facies with planktonic foraminifera and roveacrinids in the outer ramp.

foraminifera, but rudists and other taxa were not described nor recorded. Therefore, features of depositional settings in those studies contain missing data for the Derdere and Karababa formations. These units have recently been studied in southeast Turkey by Cros et al. (1999), Mülayim et al. (2018, 2019) and Özkan and Altıner (2018), who proposed a carbonate ramp process; this shows some resemblances with that of the Sabunsuyu section. However, rudist–bearing limestones were not clearly indicated and determined by those authors; our own observations have documented the presence of identifiable rudists in the same area (Yılmaz et al., 2019; Özer et al., 2019a, b). The lithological and depositional features of the Sabunsuyu section, such as the upper Cenomanian rudist–bearing, platform–type carbonates and the Turonian pelagic condensed limestone sequence, show clear similarities to those of the İnişdere section in southeast Turkey, recently presented by Mülayim et al. (2019). The presence of a hardground surface between the upper Cenomanian rudist–bearing limestones and the Turonian pelagic limestones in the Sabunsuyu section can be compared with the "drowning unconformity" of the İnişdere section of Mülayim et al. (2019), thus illustrating the same change in depositional conditions. A similar hiatus has been recorded from the Arabian Plate (Sharland et al., 2001; Haq and Al–Qahtani, 2005; Haq, 2014) and also Egypt (Bauer et al., 2003). The Bey Dağları Carbonate Platform (BDCP; southwest Turkey) comprises middle–upper Cenomanian rudist–bearing limestones as well. However, the BDCP succession differs from the Sabunsuyu sequence as the Cenomanian rudist–bearing limestones of the former do not show any pelagic incursion and are overlain by Turonian rudist–bearing neritic limestones in the northern part (Sarı et al., 2004, 2009; Sarı, 2006b; Sarı and Özer, 2009), where Turonian neritic limestones are overlain by Coniacian–Santonian pelagic limestones with planktonic foraminifera (Sarı, 2006a, 2009). However, neritic conditions prevailed throughout the Late Cretaceous in the southern part of the platform (Susuzdağ area), which includes Santonian–lower Campanian rudist–bearing limestones (Sarı et al., 2009; Sarı and Özer, 2009) which could be correlated with the Santonian rudist–bearing limestones of the Sabunsuyu succession.

The upper Cenomanian rudist–bearing limestones of the Sabunsuyu section show similarities to those of Jordan (Schulze et al., 2003, 2004; Bandel and Salameh, 2013; Özer and Ahmad, 2015, 2016), Egypt (Bauer et al., 2004; Salama et al., 2016; Farouk et al., 2017; Abdel–Fattah et al., 2018) and Tunisia (Razgallah et al., 1994; Chikhi–Aouimeur et al., 2006). However, the Turonian limestones of the Sabunsuyu section differ from those of the Afro–Arabian platform (Syria, Iraq, Jordan, Iran, Egypt, Tunisia) in the absence of rudists.

6.2. Platform–type ramp

The distribution of microfacies is presented in Fig. 10. Microfacies characteristics have allowed a good understanding of the Cenomanian–Santonian carbonate platform type, as explained below:

Pithonellid and planktonic foraminifera–rich accumulations of Mf–1 are closely associated with fine–grained carbonates deposited in an outer ramp environment, likely below normal wave base, under very low–energy conditions, suggesting that these

Fig. 9. Photomicrographs of microfacies types. A. MF–1, laminated/non–laminated silt–bearing limy mudstone, Derdere Formation, TPAO, sample 2–1. B. MF–1, laminated/non–laminated silt–bearing lime mudstone, Karababa Formation, TPAO, sample 75.1. C. MF–2, bioclastic wackestone/packstone, Derdere Formation, TPAO, sample 53.2, D. MF–3, bivalve and roveacrinid floatstone, Derdere Formation, TPAO, sample 53.4. E. MF–3, bivalve and roveacrinid floatstone, Derdere Formation, TPAO, sample 72.3. F. MF–4, echinoderm bioclastic packstone, Karababa Formation, TPAO, sample 2KB. G–H. MF–5, rudist floatstone/rudstone, Derdere Formation, TPAO, samples 70.2 and 2KB, respectively. Scale bar equals 0.5 mm. Abbreviations: TPAO – Turkish Petroleum Corporation; c – calcisphere; r – roveacrinid; b – bivalve; e – echinoid; g – gastropod; s – silty quartz grains; bc – bioclast; rd – rudist; p – pellet.

microfacies can be considered to be equivalent to RMF–5 of Flügel (2010). Skeletal grains (roveacrinids, bivalves) are commonly well preserved. The presence of a micrite matrix is evidence of a low–energy environment. Some parts of this microfacies are laminated limy mudstone with silty quartz grains of Mf–1 and could be interpreted to have formed in the proximal parts of outer–ramp settings (Flügel, 2010) below the SWB and corresponding to RMF–1 of Flügel (2010). Mf–2 could have formed between the proximal parts of mid– to outer–ramp settings and corresponds to RMF–3 of Flügel (2010). The bioclastic peloidal wackestone and packstone have abundant and diverse fossils (bivalves, gastropods, roveacrinids) and peloids. Mf–3 could have formed in open inner ramp to mid–ramp settings and corresponds to RMF–15 of Flügel (2010). Skeletal grains often are worn. Bivalve and roveacrinid floatstones are ramp–derived bioclasts, their remains embedded in a micritic matrix. Mf–4 could have formed protected and low–energy inner ramp settings and corresponds to RMF–7 of Flügel (2010). Echinoderm bioclastic packstone composed of few dominant skeletal grains (e.g., predominantly echinoderms and foraminifera). The rudist shells of Mf–5 could illustrate mid–ramp crest settings and corresponds to RMF–28 of Flügel (2010). The rudist floatstone and rudstone exhibit a strongly disorganised fabric. The occurrence of rudists and lithological and microfacies characteristics of this succession indicate that the limestones were deposited in mid– to outer–ramp environments such as described from the Arabian Platform.

7. Sequence stratigraphy

On different scales the various sequences may have resulted from fluctuating eustatic sea levels and local tectonics. The hardground surfaces recorded during fieldwork (i.e., ferruginous hard crusts), combined with vertical facies evolution, are here used to interpret sequence boundaries (SB). Moreover, major facies shifts from shallower– to deeper–marine carbonate facies indicate sequence boundaries. In total, three sequence boundaries have been identified in this succession; two in the Cenomanian (SB Ce 1–2) and one in the Turonian (SB Tu 1). These unconformities define a corresponding number of 3rd–order depositional sequences (*sensu* Posamentier et al., 1988; Vail et al., 1991) that commonly consist only of transgressive (TST) and highstand systems tracts (HST) due to a lack of accommodation space during falling and low sea level stands. Mülayim et al. (2016) were the first to interpret Cenomanian–Turonian transgressive–regressive (T–R) sedimentary cycles in the Çemberlitaş oilfield (Adıyaman, southeast Turkey), considering mainly the Cenomanian–lower Campanian interval. Sequence–stratigraphical studies in other parts of southeast Turkey include those of Tardu (1991) and Özkan and Altıner (2018). In the study area, we have subdivided the Cenomanian–Santonian succession into three sequences (Fig. 11).

7.1. Depositional sequence 1

In the outcrop studied, the base of Sequence 1 (SB 1) is the upper Albian–middle Cenomanian boundary. This sharp boundary separates the upper Albian–lower Cenomanian Sabunsuyu Formation (very thick dolomitic beds) from the overlying middle–upper Cenomanian Derdere Formation (thinner limestone and calcareous shale beds). This sequence is delineated at the base by the middle–upper Cenomanian sequence boundary (SB 1), where it is overlain by levels with *Asterohedbergella asterospinosa* of middle–late Cenomanian age. The basal sequence boundary (SB 1) is the unconformity between the Sabunsuyu and Derdere formations. This unconformity is characterised by the presence of a sudden facies shift from dolomites to limestone and by the presence of dissolution vugs indicating exposed conditions. In the Cenomanian succession exposed at Kilis (southeast Turkey), the correlative upper Albian–middle Cenomanian boundary has already been identified by Cros et al. (1999). The TST facies is composed mainly of outer–ramp facies (MF–1, laminated/non–laminated, silt–bearing limy mudstone). The transgressive system tract is marked by a small influx of siliciclastics that consist of calcareous shale with exogyrine oysters. In the Sabunsuyu section, the HST is composed mainly of limy mudstone and dolostone facies, intercalated with chert bands and nodules. The upper part is represented by aggradational stacking of shallow–ramp facies with quartz–dominated inputs in subfacies. It is marked by the presence of intensive dissolution and dolomitisation. The dolostone package resulted from aggradation when accommodation space was filled as rapidly as it was created so that water depth remained relatively constant.

7.2. Depositional sequence 2

This sequence is bounded at the base by sequence boundary 2 (SB 2), which is characterised by the presence of rudist rudstone facies. Aggradational to progradational stacking patterns identify the HST in sequence 2. During the HST, the first rudist–bearing cycle formed and prograded basinwards. The HST of the large–scale sequence 2 represents the second rudist–bearing cycle during aggradation of the carbonate ramp. The rudist–bearing cycles are identified within this systems tract and go through an ideal vertical shallowing upwards from slightly low–energy to high–energy mid–ramp facies. Petrographic descriptions for this systems tract show that it comprises two shallowing–upward parasequences. The first rudist–bearing cycle was laid down during progradation and consists of limestone with planktonic foraminifera and roveacrinids, shallowing up into rudist rudstone with benthic foraminifera and gastropods, forming the upper medium–scale sequence. The rudist assemblage in HST of the Sabunsuyu section includes *Sauvagesia* sp., *Durania* sp., *Biradiolites* sp., *Durania acuticostata, Sauvagesia sharpei* and *Bournonia*? sp. The second rudist–bearing cycle consists of limestone with echinoids and roveacrinids followed by massive rudist–bearing limestone stacked in an aggrading pattern. The foraminifera include *Meandrospira* sp., *Dorothia* sp., Gavelinellidae and Lenticulinidae; associated are bivalves and gastropods, all reflecting deposition in shallow water during the HST of sequence 2. In the Sabunsuyu section *Caprinula* sp. (*C.* cf. *sharpei*), *Sauvagesia* sp., *Radiolites* sp. and *Ichthyosarcolites triangularis* are in the HST of the upper sequence 2. The capping rudstone in both rudist–bearing cycles formed under decreased water depths due to either aggradational growth of the rudist lithostrome and/or a sea level fall. The transition from progradational early highstand to aggradational late highstand is recorded by a hardground surface at the top of a massive rudist–bearing limestone. The rudist accumulation was able to keep up with the increase in accommodation during early highstand sea level rise. The TST facies begins with bioclastic packstone in the Sabunsuyu section. These facies are overlain by quiet, open rudist floatstone/rudstone facies, which is intercalated with bioclastic wackestone. The MFS is at the top of a highly fossiliferous limestone bed with roveacrinids, echinoids, pithonellids and planktonic foraminifera, that indicate relatively deeper mid– to outer–ramp environments.

7.3. Depositional sequence 3

Sequence boundary 3 lies at the base of Sequence 3 between the middle–upper Cenomanian Derdere Formation and the Turonian–Santonian Karababa Formation. These deposits comprise

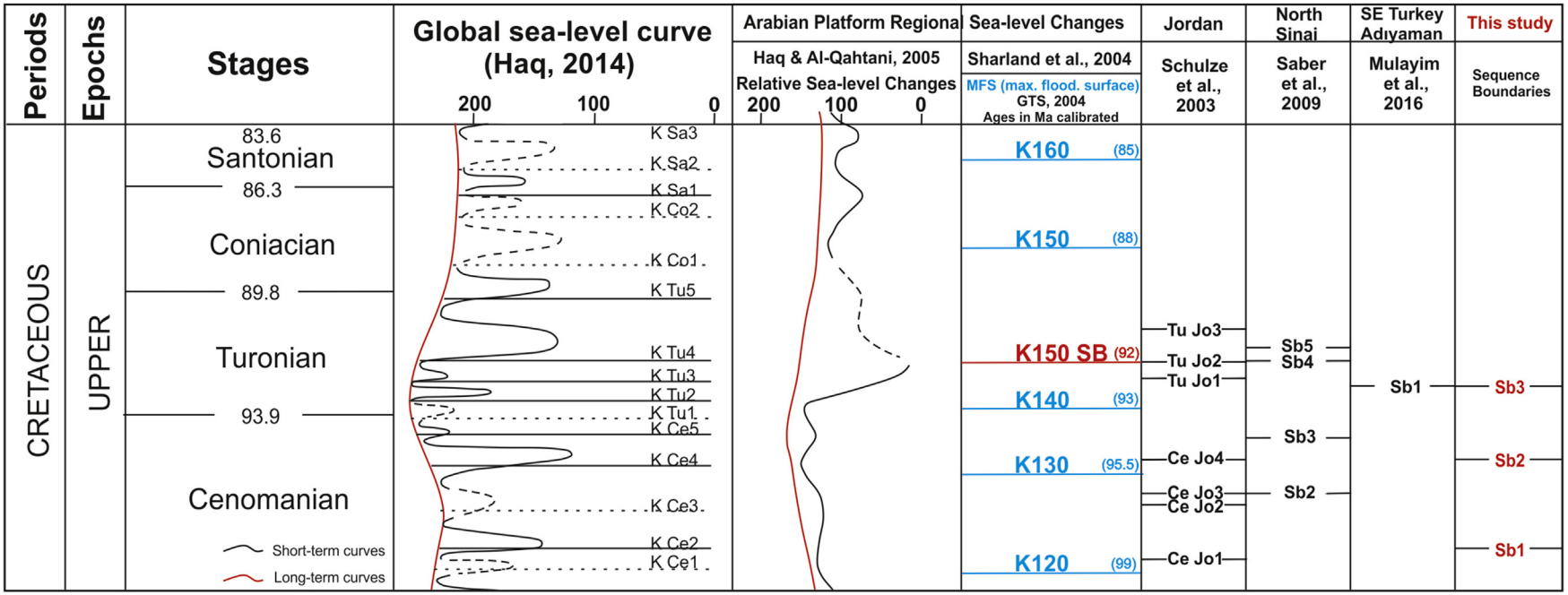

Fig. 11. Comparison between sequence boundaries of the present study with others in neighbouring areas and with the global eustatic scheme of Haq (2014).

the TST of Sequence 3 and are characterised by glauconite, pinkish iron crust and bioturbation which indicate condensation. In the Sabunsuyu section, the boundary is distinguished by a hardground. The transgressive systems tract is marked by mid– to outer–ramp deposits of limestone containing pithonellid and planktonic foraminifera. The drowning of the platform during the early Turonian is interpreted to be the result of a longer–term relative sea level rise. During the TST, acceleration in the rate of relative sea level rise led to the deposition of a retrogradational component rich in planktonic foraminifera, pithonellids and roveacrinids of mid– to outer–ramp environments. The change from TST to HST is represented by the transition from retrogradational to progradational sedimentation patterns. The maximum flooding surface in this large–scale sequence is best placed at the top of the mid– to outer –ramp facies of the maximum flooding interval.

The highstand systems tract is composed of a shallowing–upwards (prograding) parasequence set that formed due to normal regression during a sea level highstand. The relative fall/still stand in sea level led to formation of late HST deposits with shoal facies prograding basinwards. Thus, the HST is characterised by a predominance of high–energy packstone and rudist rudstone facies, which contain numerous skeletal fragments (i.e., *Bournonia excavata*, *Apricardia* sp. and indeterminate bivalves). The HST deposits are mainly peloid silty bioclastic packstone and echinoderm/benthic foraminifera–bioclastic packstone intercalated with mudstone. These bioclastic packstones, interpreted as storm layers (Aigner, 1985), are common but usually amalgamated with wavy beds of graded bioclastic material. In fact, during these phases of base–level highstand, these deposits contain numerous echinoids which indicate a change from moderate energy of the mid–ramp to high–energy shoal facies.

7.4. Sequence–stratigraphical comparison

The sequence–stratigraphical framework of the middle–upper Cenomanian–Santonian succession in the Sabunsuyu section has been compared with schemes proposed by Schulze et al. (2003), Sharland et al. (2004), Haq and Al–Qahtani (2005), Saber et al. (2009), Haq (2014) and Mülayim et al. (2016) (Fig. 11). Their correlation incorporates the stratigraphical succession of the Sabunsuyu section and positions of the SBs recognised in the study area.

Depositional sequence 1 is the thickest sequences in the middle to upper Cenomanian of the Sabunsuyu section. We interpret this thickness increase to reflect prolonged duration of the sea level in highstand position on the Arabian Platform due to a 2nd–order rise of sea level from the middle to late Cenomanian (Haq, 2014). Thus, this global signal probably controlled the sedimentation rate in this time interval and carbonate production increased in the outer– to mid–ramp highstand carbonate deposits (Mülayim et al., 2016). Despite the thickness reduction and the effect of dolomitisation which masked the original depositional texture and composition of the depositional sequences in the Cenomanian, palaeontological data for depositional sequence 1 have enabled us to correlate with Haq (2014) and recognise the middle Cenomanian sequence boundary (SB2) in the study area. This is also correlated with SB2 in northern Sinai (Saber et al., 2009), CeJo3 in Jordan (Schulze et al., 2003, 2005) and KCe4 of Haq (2014) (Fig. 11). Following the mid–Cenomanian regression, sea–level rise during the late Cenomanian and early Turonian led to deposition of transgressive systems tract of the second sequence. This system tract is characterised mainly by mid–outer ramp facies rich in planktonic foraminifera and calcispheres. Depositional sequence 2, well exposed in the field, displays evolution from outer– to mid–ramp deposition and is abruptly overlain by pelagic deposits of the Karababa A and B members, signalling changing rates of subsidence in the Arabian Platform and the onset of tectonic events. The upper Cenomanian–lower Turonian transgression is assumed here to correlate with the eustatic sea–level rise of Haq (2014) and regional deeping in the adjacent shelf area in Jordan (Schulze et al., 2003, 2005) and the Arabian Peninsula (Sharland et al., 2001). The upper part of this facies (late Cenomanian) was considered by Mülayim et al. (2016, 2019) to reflect the Oceanic Anoxic Event 2 (OAE 2) in the İnişdere and Türkoğlu sections.

8. Conclusions

Rudists are here described from the Sabunsuyu succession for the first time. The biostratigraphical data obtained from these provide a valuable contribution to a better understanding of the Derdere and Karababa formations in the Sabunsuyu succession.

Rudists and microfacies characteristics of the limestones provide data on the depositional environments of the Cenomanian–Santonian succession, revealing that the limestones formed on an inner to outer homoclinal ramp of (a) carbonate platform(s). Rudists formed small isolated patches and aggregations in a mid–ramp environment and were commonly deposited as shell fragments particularly on the outer ramp in response to increasing energy and ramp slope characteristics.

Monospecific tabular beds mainly characterise the upper intervals and, together with features described above, are indicative of shallow–water depositional environments that were subjected to periodical input of planktonic levels and influenced by storm events. The increase upsection of more complex rudist concentrations characterised by moderate species diversity, together with the disappearance of emersion surfaces and the storm and/or wave intercalations, record a general deepening–upwards trend and more open–water conditions.

Rudist–dominated facies developed in the Derdere and Karababa formations during the deposition of three sequences in the Sabunsuyu section. Most rudist facies dominate in the HST phase. The HST phase of sequence 2 is characterised by the presence of *Sauvagesia* sp., *Durania* sp., *Biradiolites* sp., *Durania acuticostata*, *Sauvagesia sharpei* and *Bournonia*? sp., *Caprinula* sp. (*C.* cf. *sharpei*), *Radiolites* sp., *Ichthyosarcolites triangularis* and *Neithea fleuriausiana*, indicating a late Cenomanian age. The Derdere Formation comprises poor planktonic foraminiferal assemblages, including *Asterohedbergella asterospinosa* which is characteristic of the middle to upper Cenomanian. The rudist fauna of the Karababa Formation, characterised by the abundance of *Bournonia excavata*, is dated as Coniacian–Santonian. The biogeography and correlation of rudists identified here show a low diversity in comparison to those of the northern Mediterranean Tethys, but are similar to recorded occurrences from the southern margin and to the distribution and diversity of these species towards the eastern part of the Arabian Platform. The Cenomanian–Turonian carbonate ramp in the study area was dominated by rudists (Radiolitidae and Ichthyosarcolitidae), being the most significant benthic carbonate producers, mainly in highstand systems tracts of sequences 1, 2 and 3.

A comparison of the sequence–stratigraphical framework with that for adjacent areas (northern Sinai, Gulf of Suez and Jordan) and with the global scheme of Haq (2014) reveals a few differences in timing of sequence boundaries, which may be related mainly to local/regional tectonic events that affected deposition in the study area, as well as to minor sea–level fluctuations. It is concluded here that the depositional history of the Cenomanian–Turonian sequence examined was controlled by global eustatic sea level change (Haq and Al–Qahtani, 2005; Haq, 2014) and a regional to local tectonic effect (i.e., trusting and crustal loading) of the development in the northern Arabian continental margin in

southeast Turkey that began during the late Cenomanian–early Turonian.

Declaration of competing interest

The authors declare that they have no competing interests.

CRediT authorship contribution statement

Oğuz Mülayim: Conceptualization, Methodology, Formal analysis, Investigation, Validation, Visualization, Writing - original draft, Writing - review & editing. **İsmail Ömer Yılmaz:** Conceptualization, Methodology, Formal analysis, Supervision, Validation, Visualization, Resources, Writing - review & editing. **Sacit Özer:** Conceptualization, Formal analysis, Supervision, Validation, Investigation, Visualization, Writing - review & editing. **Bilal Sarı:** Resources, Writing - review & editing. **Kemal Taslı:** Resources, Writing - review & editing.

Acknowledgments

This work was partially supported by the Scientific and Technological Research Council of Turkey (TUBITAK, Project no. 118Y425, Ankara, Turkey). We would like to thank TPAO for logistic support and are grateful to Robert Scott and two anonymous reviewers, as well as Eduardo Koutsoukos (Editor–in–Chef) and John Jagt (Handling Editor), for corrections and comments on previous versions of the text.

References

Abdallah, H., 2003. Genesis and diagenesis of the Gattar carbonate platform, lower Turonian, northern southern Tunisia. In: Gili, E., Negra, H., Skelton, P.W. (Eds.), North African Cretaceous carbonate platform systems. NATO Science Series 28, pp. 31–51.

Abdel–Fattah, Z.A., Kora, M.A., Raafat, S.A., 2018. Depositional environments and sequence stratigraphy of a mixed siliciclastic–carbonate ramp. An example from the Cenomanian to Turonian Galala Formation in the northern Eastern Desert, Egypt. Journal of African Earth Sciences 147, 352–373.

Aigner, T., 1985. Storm depositional systems. Dynamic stratigraphy in modern and ancient shallow marine sequences. Springer, Berlin, p. 174.

Aksu, R., Mutlu, R., Utmanoğulları, M., Tofan, R., 2014. Gaziantep batısı Burç–Musabeyli– Sakçagöz arasının jeolojisi. XI–XII bölge sorumluluğu. Sunum, TPAO Ankara.

Alsharhan, A.S., Nairn, A.E.M., 1997. Sedimentary basins and petroleum geology of the Middle East. Elsevier, Amsterdam, p. 878.

Bandel, K., Salameh, H., 2013. Geologic development of Jordan. Evolution of its rocks and life. The University of Jordan Press, Amman, p. 278.

Bauer, J., Marzouk, A.M., Steuber, T., Kuss, J., 2001. Lithostratigraphy and biostratigraphy of the Cenomanian–Santonian strata of Sinai, Egypt. Cretaceous Research 22, 497–526.

Bauer, J., Kuss, J., Steuber, T., 2003. Sequence architecture and platform configuration (Late Cenomanian–Santonian), Sinai, Egypt. Sedimentology 50, 387–414.

Bauer, J., Steuber, T., Kuss, J., Heimhofer, U., 2004. Distribution of shallow–water benthics (rudists, calcareous algae, benthic foraminifera) in the Cenomanian–Turonian carbonate platform sequences of Sinai, Egypt. In: Hofling, R. (Ed.), Contributions to the 5th International Congress on Rudists, Erlangen, Germany 1999, vol. 247. Courier Forschungsinstitut Senckenberg, pp. 207–232.

Bayle, E., 1857. Nouvelles observations sur quelques especes de rudistes. Bulletin de la Societe geologique de France 2 (14), 647–719.

Bonet, F., 1956. Zonificación Microfaunística de las Calizas Cretácicas del Este de México: Boletín de la Asociación Mexicana de Geólogos Petroleros 8 (7–8), 389–488.

BouDagher–Fadel, M.K., 2012. Biostratigraphic and geological significance of planktic Foraminifera [Developments in Palaeontology and Stratigraphy 22. Elsevier, Amsterdam, p. 312.

Caffau, M., Pugliese, N., Plenicar, M., 1996. The development of the mollusc fauna in the Cenomanian of the stratigraphic sequence of Visogliano (Karst of Triest, Italy). Geologija 37/38 (for 1994/1995), 87–121.

Carbone, F., 1993. Cretaceous depositional systems of the evolving Mesozoic carbonate platform of central Apennine thrust belt, Italy. Geologica Romana 29, 31–53.

Carbone, F., Praturlon, A., Sirna, G., 1971. The Cenomanian shelf edge facies of Rocca di Cave. Geologica Romana 10, 131–197.

Çelikdemir, E.M., Dülger, S., Görür, N., Wagner, C., Uygur, K., 1991. Stratigraphy, sedimentology, and hydrocarbon potential of the Mardin Group, SE Turkey. Special Publications of the European Association of Petroleum Geoscientists 1, 439–454.

Cestari, R., 2008. Los rudistas (Bivalvia, Hippuritoidea) en el Appenino centro–meridional (Italia): análisis de las associaciones de Radíolitidos en contexto de plataforma calcárea en el Super–Greenhouse climate del Cretácico Superior. Unpubl. PhD thesis. Universitat Autònoma de Barcelona, Bellaterra, p. 198.

Cestari, R., Laviano, A., 2012. Rudist facies distribution in the Late Cretaceous of Cilento and western Basilicata (southern Italy). Rivista Italiana di Paleontologia e Stratigrafia 118, 277–294.

Cestari, R., Sartorio, D., 1995. Rudists and facies of the periadriatic domain. Agip, S. Donato Milanese, p. 207.

Cestari, R., Pons, J.M., Sirna, G., 1998. Undescribed *Ichthyosarcolites* from Sicily belonging to Gemmellaro's Collection. In: Masse, J.–P., Skelton, P.W. (Eds.), Quatrième Congrès international sur les Rudistes. Géobios, Mémoire spécial 22, pp. 69–73.

Chikhi–Aouimeur, F., 2010. L'Algerié à travers son patrimoine paléontologique. Les rudistes. Sarl Baosem, p. 269.

Chikhi–Aouimeur, F., Abdallah, H., Pons, J.–M., Vicens, E., 2006. The Cenomanian–Turonian rudists of the Gafsa region, Tunisia. In: Malchus, N., Pons, J.–M. (Eds.), Organisms diversity and evolution 6. Electronic supplement 16, Abstracts and posters of the "International Congress on Bivalvia" at the Universitat Autònoma de Barcelona, Spain, 22–27 July 2006.

Choffat, P., 1885. Recueil des monographies stratigraphiques sur la systeme cretacique du Portugal. 1. Etude. Contrees de Cintra, de Bellas et de Lisbonne 1–68.

Çoruh, T., Yakar, H., Ediger, V.S., 1997. Güneydoğu Anadolu Bölgesi otokton istifinin biyostratigrafi atlası (Atlas of biostratigraphy for the autochthonous succession of the southeastern Anatolian Region). TPAO Araştırma Merkezi Grubu, Eğitim Yayınları, Ankara 30, 401.

Cros, P., Dercourt, J., Günay, Y., Fourcade, É., Bellier, J.–P., Lauer, J.P., Manivit, H., Kozlu, H., 1999. The Arabian Platform in southeastern Turkey: an Albian–Cenomanian carbonate ramp collapsed during the Senonian. TAPG Bulletin 11 (1), 55–77.

d'Orbigny, A., 1842. Quelques considerations géologiques sur les rudistes. Bulletin de la Société géologique de France 1 (13), 148–159.

d'Orbigny, A., 1847. Sur les brachiopodes ou palliobranches. Comptes Rendus hebdomadaires des Séances de l'Académie des Sciences Paris 25, 266–269.

d'Orbigny, A., 1850. Paléontologie Française, Terrains crétacés 4, Brachiopodes. Masson, Paris, pp. 105–328.

Desmarest, A.G., 1817. Mémoire sur deux genres de coquilles fossiles cloisonnées et à siphon. Journal de Physique, de Chimie et d'Histoire naturelle 85, 42–51.

Dhondt, A.V., 1973. Systematic revision of the subfamily Neitheinae (Pectinidae, Bivalvia, Mollusca) of the European Cretaceous. Mémoires de l'Institut royal des Sciences naturelles de Belgique 176, 1–101.

Di Stefano, P., Ruberti, D., 2000. Cenomanian rudist–dominated shelf–margin limestones from the Panormide carbonate platform (Sicily, Italy): facies analysis and sequence stratigraphy. Facies 42, 133–160.

Douvillé, H., 1888. Études sur les caprines. Bulletin de la Societe Geologique de France 16 (3), 699–730.

Dunham, R.J., 1962. Classification of carbonate rocks according to depositional texture. Bulletin of the American Association of Petroleum Geologists 1, 108–121.

El–Sabbag, A.M., Tantawy, A.A., Keller, G., Khozyemd, H., Spangenberg, J., Adatte, T., Gertsch, B., 2011. Stratigraphy of the Cenomanian–Turonian oceanic anoxic event OAE2 in shallow shelf sequences of NE Egypt. Cretaceous Research 32, 705–722.

Embry, A.F., Klovan, J.E., 1971. A Late Devonian reef tract on northeastern Banks Island, Northwest Territories. Bulletin of Canadian Petroleum Geology 33, 730–781.

Farouk, S., Ahmad, F., Powell, J.H., 2017. Cenomanian–Turonian stable isotope signatures and depositional sequences in northeast Egypt and central Jordan. Journal of Asian Earth Sciences 134, 207–230.

Flügel, E., 2010. Microfacies of carbonate rocks. Analysis, interpretation and application. Springer, Berlin, p. 976.

Frank, R., Buchbinder, B., Benjamini, C., 2010. The mid–Cretaceous carbonate system of northern Israel: facies evolution, tectono–stratigraphy configuration and global control on the central Levant margin of the Arabian plate. In: Homberg, C., Bachmann, M. (Eds.), Evolution of the Levant Margin and western Arabian platform since the Mesozoic, vol. 341. Geological Society, London, Special Publication, pp. 133–170.

Frija, G., Parente, M., Di Lucia, M., Mutti, M., 2015. Carbon and strontium isotope stratigraphy of the Upper Cretaceous (Cenomanian–Campanian) shallow–water carbonates of southern Italy: chronostratigraphic calibration of larger foraminifera biostratigraphy. Cretaceous Research 53, 110–139.

Gili, E., Götz, S., 2018. Paleoecology of rudists. Part N2, Chapter 26B. Treatise Online 103, 1–29.

Gili, E., Masse, J.–P., Skelton, P.W., 1995. Rudists as gregarious sediment–dwellers, not reef–builders, on Cretaceous carbonate platforms. Palaeogeography, Palaeoclimatology, Palaeoecology 118, 245–267.

Görür, N., Akkök, R., Yöndem, F., Sarıdaş, B., 1981. Sabunsuyu–II ölçülmüş kesiti. TPAO Arama Grubu. Arşiv no. 9244.

Görür, N., Çelikdemir, E., Dülger, S., 1991. Carbonate platforms developed on passive continental margins: Cretaceous Mardin carbonates in southeast Anatolia as an example. Bulletin of the Technical University of Istanbul 44, 301–324.

Gül, M.A., Kaya, İ.H., Selvi, B., Yıldızel, A., Erenler, M., Günal, B., İllezz, H.İ., Ulu, M., Aköz, Ö., Akça, N., Ertuğ, K., 2001. Gaziantep–Kilis–Hatay civarının stratigrafik ve jeokimyasal incelemesi ve Bölgenin Jeolojik Evrimi, p. 214. TPAO–ARGEM, rapor no. 2617.

Güven, A., Dinçer, A., Tuna, M.E., Tezcan, Ü.Ş., Çoruh, T., 1988. Güneydoğu Anadolu'da Mardin ve Midyat Grupları arasında yer alan birimlerin stratigrafisi (ön rapor), p. 154. TPAO Arama Grubu, Rapor no. 2414.

Hajikazemi, E., Al–Aasm, I.S., Coniglio, M., 2010. Subaerial exposure and meteoric diagenesis of the Cenomanian– Turonian Upper Sarvak Formation, southwestern Iran. Geological Society, London, Special Publications 330, 253–272.

Hamaoui, M., 1965. On a new subgenus of *Hedbergella* (Foraminiferida). Israel Journal of Earth Sciences 13, 133–142.

Haq, B., 2014. Cretaceous eustasy revisited. Global and Planetary Change 113, 44–58.

Haq, B., Al–Qahtani, A.M., 2005. Phanerozoic cycles of sea–level change on the Arabian Platform. GeoArabia 10, 127–160.

Harris, P.M., Frost, S.H., Seigle, G.A., Schneidermann, N., 1984. Regional unconformities and depositional cycles, Cretaceous of the Arabian Peninsula. In: Schlee, J.S. (Ed.), International unconformities and hydrocarbon accumulation. American Association of Petroleum Geologists Memoir 36, pp. 67–80.

Keskin, C., Tuna, D., Güneri, Y., 1974. Sabunsuyu normal kesiti. TPAO Arama Grubu, Arşiv no. 6254.

Khazaei, A.R., Skelton, P.W., Yazdi, M., 2010. Maastrichtian rudist fauna from Tarbur Formation (Zagros region, SW Iran). Preliminary observations. In: Özer, S., Sarı, B., Skelton, P.W. (Eds.), Jurassic–Cretaceous rudists and carbonate platforms, Part (A), 8th International Rudist Congress, vol. 19. Turkish Journal of Earth Sciences, pp. 703–719.

Korbar, T., Fuček, L., Husinec, A., Vlahović, I., Oštrić, N., Matičec, D., Jelaska, V., 2001. Cenomanian carbonate facies and rudists along shallow intraplatform basin margin –the Island of Cres (Adriatic sea, Croatia). Facies 45, 39–58.

Kuss, J., Bassiouni, A., Bauer, J., Bachmann, M., Marzouk, A., Scheibner, C., Schulze, F., 2003. Cretaceous–Paleogene sequence stratigraphy of the Levant Platform (Egypt, Sinai, Jordan). In: Gili, E., Negra, H., Skelton, P.W. (Eds.), North African Cretaceous carbonate platform systems. NATO Science Series 28, pp. 171–187.

Laviano, A., Maresca, M.G., Tropeano, M., 1998a. Stratigraphic organization of rudist biogenic beds in the Upper Cenomanian successions of the western Murge (Apulia, southern Italy). In: Masse, J.–P., Skelton, P.W. (Eds.), Quatrième Congrès International sur les Rudistes. Géobios, Mémoire Speciale 22, pp. 159–168.

Laviano, A., Sirna, G., Facchini, G., 1998b. Rudist facies distribution in the central–southern Apennines and Apulia, Italy. In: Masse, J.–P., Skelton, P.W. (Eds.), Quatrième Congrès International sur les Rudistes. Géobios, Mémoire Speciale 22, pp. 169–180.

Loeblich Jr., A.R., Tappan, H., 1988. Foraminiferal genera and their classification. Van Nostrand Reinhold Company, New York, p. 970.

Lorenz, T., 1902. Geologische Studien in Grenzgebiete zwichen helvetischer und ostalpiner Fazies II. Teil. Südlicher Rhaetikon: Berichte der Naturforschenden Gesellschaft zu Freiburg im Breisgau 12, 34–62.

Lucena Santiago, G., 2014. Revisión de la fauna de rudistas de les Collades de Basturs (Lleida, Pirineos Centro–Meridionales). Unpubl. PhD thesis. Universitat Autònoma de Barcelona, Bellaterra, p. 290.

Macé–Bordy, J., 2007. Révision des rudistes crétacés (Bivalvia) de la Paléontologie Française d'Alcide d'Orbigny. Deuxième partie. Annales de Paléontologie 93, 67–105.

Mülayim, O., Mancini, E., Çemen, İ., Yılmaz, İ.Ö., 2016. Upper Cenomanian–Lower Campanian Derdere and Karababa formations in the Çemberlitaş oil field, southeastern Turkey: their microfacies analyses, depositional environments, and sequence stratigraphy. Turkish Journal of Earth Sciences 25, 46–63.

Mülayim, O., Yilmaz, I.Ö., Ferré, B., 2018. Roveacrinid microfacial assemblages (Roveacrinida, Crinoidea) from the Lower–Middle Cenomanian of the Adıyaman area (SE Turkey). Arabian Journal of Geosciences 11, 545. https://doi.org/10.1007/s12517–018–3901–z.

Mülayim, O., Yilmaz, O.I., Sarı, B., Taslı, K., Wagreich, M., 2019. Cenomanian–Turonian drowning of the Arabian Carbonate Platform, the İnişdere section, Adıyaman, SE Turkey. In: Wagreich, M., Hart, M.B., Sames, B., Yilmaz, I.O. (Eds.), Cretaceous climate events and short–term sea–level changes. Geological Society of London, Special Publication. https://doi.org/10.1144/SP498–2018–130.

Okay, A.I., 2008. Geology of Turkey: a synopsis. Der Anschnitt 21, 19–42.

Özer, S., 1988. Descriptions de quelques rudistes à canaux dans le Cénomanien de Turquie. Géologie Méditerraneanne 15, 159–167.

Özer, S., 2005. Two new species of canaliculate rudists (Dictyoptychidae) from southeastern Turkey. Geobios 38, 235–245.

Özer, S., 2010a. *Dictyoptychus* Douvillé: taxonomy, revision, phylogeny and biogeography. In: Özer, S., Sarı, B., Skelton, P.W. (Eds.), Jurassic– Cretaceous rudists and carbonate platforms, Part (A), 8th International Rudist Congress, vol. 19. Turkish Journal of Earth Sciences, pp. 583–612 (5).

Özer, S., 2010b. Campanian–Maastrichtian *Pseudosabinia* from Turkey: descriptions and taxonomic problems. In: Özer, S., Sarı, B., Skelton, P.W. (Eds.), Jurassic–Cretaceous rudists and carbonate platforms, Part (A), 8th International Rudist Congress, vol. 19. Turkish Journal of Earth Sciences, pp. 643–669 (5).

Özer, S., Ahmad, F., 2015. Cenomanian–Turonian rudist (Bivalvia) lithosomes from NW of Jordan. Journal of African Earth Sciences 107, 119–133.

Özer, S., Ahmad, F., 2016. *Caprinula* and *Sauvagesia* rudist faunas (Bivalvia) from the Cenomanian of NW Jordan. Stratigraphy and taxonomy. Cretaceous Research 58, 141–159.

Özer, S., El–Sorogy, A.S., 2017. New record of *Durania cornupastoris* (rudist) from the Campanian of the Aruma Formation, Riyadh, Saudi Arabia: description and biogeographic remarks. Journal of African Earth Sciences 129, 380–389.

Özer, S., Kahrıman, H.H., 2019. Cenomanian canaliculated rudists (Bivalvia) from the Geyik Dağı–Hadim area (Central Taurides, S Turkey): systematic paleontology, stratigraphic importance and depositional environments. Cretaceous Research 104161. https://doi.org/10.1016/j.cretres.2019.06.007.

Özer, S., Meriç, E., Görmüş, M., Kanbur, S., 2009. Biogeographic distributions of the rudists and benthic foraminifera: an approach to Campanian–Maastrichtian paleobiogeography of Turkey. Geobios 42, 623–638.

Özer, S., Karim, K.H., Sadiq, D.M., 2013. First determination of rudists (Bivalvia) from NE Iraq: systematic palaeontology and palaeobiogeography. Bulletin of the Mineral Research and Exploration 147, 31–55.

Özer, S., El–Sorogy, A.S., Al–Dabbagh, M.E., Al–Kahtany, K., 2019a. Campanian–Maastrichtian unconformities and rudist diagenesis, Aruma Formation, Central Saudi Arabia. Arabian Journal of Geosciences 12, 1–17.

Özer, S., Yilmaz, I.O., Mülayim, O., Sarı, B., Hoşgör, I., Tasli, K., 2019b. Upper Cretaceous rudist carbonate ramp facies in the SE Anatolia, Turkey: a comparison with the Arabian platform facies. In: 34th IAS Meeting of Sedimentology Conferences, Roma, Italy, p. 27.

Özkan, R., Altıner, D., 2018. The Cretaceous Mardin Group carbonates in southeast Turkey: lithostratigraphy, foraminiferal biostratigraphy, microfacies and sequence stratigraphic evolution. Cretaceous Research 98, 153–178.

Parente, M., Frijia, G., Di Lucia, M., 2007. Carbon–isotope stratigraphy of Cenomanian– Turonian platform carbonates from the southern Apennines (Italy): a chemostratigraphic approach to the problem of correlation between shallow–water and deep–water successions. Journal of the Geological Society London 164, 609–620.

Perinçek, D., Duran, O., Bozdoğan, N., Çoruh, T., 1991. Stratigraphy and paleogeography evolution of the autochthonous sedimentary rock in the SE Turkey (Güneydoğu Türkiye'de otokton sedimanter kayaların stratigrafisi ve paleocoğrafik evrimi). Ozan Sungurlu Symposium Proceedings 274–305.

Philip, J., 1980. Crétacé supérieur de Provence. Géobios. Mémoire Spécial 4, 99–109.

Philip, J., Mermigis, A., 1989. Bioconstructions et plates–formes carbonatées à rudistes du Crétacé supérieur des zones ophiolitiques: le Massif de l'Akros (Argolide, Grèce). Geologie Mediterraneenne 16, 145–153.

Philip, J., Babinot, J.–F., Tronchetti, G., Fourcade, E., Ricou, L.–E., Guiraud, R., Bellion, Y., Herbin, J.–P., Combes, P.–J., Cornee, J.–J., Dercourt, J., 2000. Late Ceonamanian. In: Dercourt, J., Gaetani, M., Vrielynck, B., Barrier, E., Biju–Duval, B., Brunet, M.F., Cadet, J.P., Crasquin, S., Sandulescu, M. (Eds.), Atlas Peri–Tethys Palaeogeographical Maps, Map 14. CCGM/CGMW, Paris.

Pleničar, M., Jurkovšek, B., 2000. Rudists from the Cenomanian bioherms of Hrusice and Nanos, Slovenia. Geologija 42, 69–116.

Polšak, A., 1967. Macrofaune crétacée de l'Istrie méridionale (Yougoslavie). Palaeontologica Jugoslavica 8, 1–219.

Pons, J.–M., Vicens, E., Tarlao, A., 2011. Cenomanian radiolitid bivalves from Malchina, Karst of Trieste, Italy. Cretaceous Research 32, 647–658.

Posamentier, H.W., Jervey, M.T., Vail, P.R., 1988. Eustatic controls on clastic deposition, I. Conceptual framework. In: Wilgus, C.K., Hastings, B.S., Kensall, C.G.S.C., Posamentier, H.W., Ross, C.A., Van Wagoner, J.C. (Eds.), Sea–level changes: an integrated approach, vol. 42. Society of Economic Paleontologists and Mineralogists, Special Publication, pp. 109–124.

Powell, J.H., 1989. Stratigraphy and sedimentation of the Phanerozoic rocks in central and south Jordan – Part B: Kurnub, Ajlun and Belqa groups. Geological Bulletin No. 11. The Hashemite Kingdom of Jordan, Ministry of Energy and Mineral Resources, Natural Resources Authority Amman, p. 130.

Razgallah, S., Philip, J., Thomel, G., Zaghbib–Turki, D., Chaabani, F., Ben Haj Ali, N., M'Rabet, A., 1994. La limite Cénomanien–Turonien en Tunisie centrale et méridionale: biostratigaphie et paléoenvironnements. Cretaceous Research 15, 507–533.

Rineau, V., Villier, L., 2018. Taxonomic revision of the genus *Ichthyosarcolites* Demarest, 1812, and description of a new canaliculate rudist from the Cenomanian of Slovenia: *Oryxia sulcata* gen. et sp. nov. (Bivalvia, Hippuritida). Cretaceous Research 90, 60–79.

Robertson, A.H.F., Boulton, S.J., Taslı, K., Yıldırım, N., Inan, N., Yıldız, A., Parlak, O., 2016. Late Cretaceous–Miocene sedimentary development of the Arabian continental margin in SE Turkey (Adıyaman region): implications for regional palaeogeography and the closure history of southern Neotethys. Journal of Asian Earth Sciences 115, 571–616.

Saber, G.S., Salama, Y.F., Scott, R.W., Abdel–Gawad, G.I., Aly, M.F., 2009. Cenomanian–Turonian rudist assemblages and sequence stratigraphy on the North Sinai carbonate shelf, Egypt. GeoArabia 14, 113–134.

Salama, Y.F., Abdel–Gawad, G.I., Saber, S.G., El–Shazly, S.H., Grammer, G.M., Özer, S., 2016. Chemostratigraphy of the Cenomanian–Turonian shallow–water carbonate: new correlation for the rudist levels from North Sinai, Egypt. Arabian Journal of Geosciences 9, 755.

Sartorio, D., Tunis, G., Venturini, S., 1992. Open circulation facies in the Cenomanian of the northeastern margin of the Friuli Platform: the Iudrio Valley Case (NE Italy). Geologia Croatica 45, 87–93.

Sarı, B., 2006a. Upper Cretaceous planktic foraminiferal biostratigraphy of the Bey Dağları autochthon in the Korkuteli area, western Taurides, Turkey. Journal of Foraminiferal Research 36, 241–261.

Sarı, B., 2006b. Foraminifera–rudist biostratigraphy, Sr–C–isotope stratigraphy and microfacies analysis of the Upper Cretaceous sequences of the Bey Dağları

Autochthon (western Taurides, Turkey). Unpubl. PhD thesis. Dokuz Eylul University, İzmir, p. 436.
Sarı, B., Özer, S., 2009. Upper Cretaceous rudist biostratigraphy of the Bey Dağları carbonate platform, western Taurides, SW Turkey. Géobios 42, 359–380.
Sarı, B., Steuber, T., Özer, S., 2004. First record of Upper Turonian rudists (Mollusca, Hippuritoidea) in the Bey Dağları carbonate platform, Western Taurides (Turkey): taxonomy and strontium isotope stratigraphy of *Vaccinites praegiganteus* (Toucas, 1904). Cretaceous Research 25, 235–248.
Sarı, B., Taslı, K., Özer, S., 2009. Benthonic foraminiferal biostratigraphy of the Upper Cretaceous (Middle Cenomanian–Coniacian) sequences of the Bey Dağları Carbonate Platform, western Taurides, Turkey. Turkish Journal of Earth Sciences 18, 393–425.
Schulze, F., Lewy, Z., Kuss, J., Gharaibeh, A., 2003. Cenomanian–Turonian carbonate platform deposits in west central Jordan. International Journal of Earth Sciences (Geologische Rundschau) 92, 641–660.
Schulze, F., Marzouk, A., Bassiouni, M.A.A., Kuss, J., 2004. The upper Albian to Turonian carbonate platform succession of west central Jordan–stratigraphy and crisis. Cretaceous Research 25, 709–737.
Schulze, F., Kuss, J., Marzouk, A., 2005. Platform configuration, microfacies and cyclicities of the upper Albian to Turonian of west–central Jordan. Facies 50, 505–527.
Scott, R.W., 1990. Models and stratigraphy of mid–Cretaceous reef communities, Gulf of Mexico. Society of Economic Paleontologists and Mineralogists, Concepts in Sedimentology and Paleontology 2, 102.
Şengör, A.M.C., Yilmaz, Y., 1981. Tethyan evolution of Turkey: a plate tectonic approach. Tectonophysics 75, 181–241.
Sharland, P.R., Archer, R., Casey, D.M., Davies, R.B., Hall, S.H., Heward, A.P., Horbury, A.D., Simmons, M.D., 2001. Arabian plate sequence stratigraphy, vol. 2. GeoArabia, Special Publication, p. 371.
Sharland, P.R., Casey, D.M., Davies, R.B., Simmons, M.D., Sutcliffe, O.E., 2004. Arabian plate sequence stratigraphy – revisions to SP2. GeoArabia 9, 199–214.
Skelton, P.W., Gili, E., 2002. Palaeoecological classification of rudist morphotypes. In: Proceedings of the 1st International Conference of Rudists, Belgrad 1988. Serbian Geological Society, Special Publication, pp. 265–287.
Slišković, T., 1966. Zwei neue Arten der Gattung *Ichthyosarcolites* aus der Oberkreide (Ablagerungen der Südherzegowina). Conseil des Académies des Sciences et des Arts de la RSF de Yougoslavie. Bulletin scientifique A12, 177–178.
Stampfli, G.M., Borel, G., Cavazza, W., Mosar, J., Ziegler, P.A., 2001. The paleotectonic atlas of the Peritethyan domain. European Geophysical Society, CD–ROM. Electronic Publishing and Consulting, Berlin.
Steuber, T., 1999. Cretaceous rudists of Boeotia, central Greece. Special Papers in Palaeontology 61, 1–229.
Steuber, T., 2002. Web Catalogue of the Hippuritoidea (rudist bivalves). http://www.paleotax.de/rudists/index.htm.
Steuber, T., Özer, S., Schlüter, M., Sarı, B., 2009. Description of *Paracaprinula syriaca* Piveteau (Hippuritoidea, Plagioptychidae) and a revised age of ophiolite obduction on the African–Arabian Plate in southeastern Turkey. Cretaceous Research 30, 41–48.
Stössel, I., Bernouilli, D., 2000. Rudist lithosome development on the Maiella carbonate platform magrin. In: Insalaca, E., Skelton, P.W., Palmer, T.J. (Eds.), Carbonate platform systems: components and interactions, vol. 178. Geological Society, London, Special Publication, pp. 177–190.
Sungurlu, O., 1974. VI. Bölge kuzey sahalarının jeolojisi, p. 32. TPAO Arama Grubu, Rapor no. 871.
Tappan, H., 1940. Foraminifera from the Grayson Formation of Northern Texas. Journal of Paleontology 17, 476–517.
Tardu, T., 1991. A sequence stratigraphic approach to the Mardin Group: tectonics and hydrocarbon potential of Anatolia and surrounding regions. In: Proceedings of Ozan Sungurlu Symposium. Turkish Association of Petroleum Geologists, Ankara, pp. 306–332.
Toucas, A., 1907. Études sur la classification et sur l'évolution des Radiolitidés. Première partie: *Agria* et *Praeradiolites*. Mémoires de la Société géologique de France 36 (14), 5–46.
Troya, L., Vicens, E., Pons, J.–M., Lucena, G., 2011. Cenomanian rudists from platform margin to lower slope settings, p. 18. Sant Gervàs–Sopeira area, south–central Pyrenees, Spain. In: The Ninth International Congress on Rudist Bivalves, 18–25 June 2011, Kingston, Jamaica. Abstracts, Articles and Field Guides.
Troya Garcia, L., 2015. Rudistas (Hippuritida, Bivalvia) del Cenomaniense–Coniaciense (Cretácico superior) del Pirineo meridional–central. Paleontologia i biostratigrafia. Unpubl. PhD thesis. Universitat Autònoma de Barcelona, Bellaterra, p. 497.
Tunis, G., Özer, S., Radoičić, R., Săsăran, L., Tarlao, A., Tentor, M., 2013. The state of the knowledge of the genus *Pseudopolyconites*. Caribbean Journal of Earth Science 45, 107–118.
Vail, P.R., Audemard, F., Bowman, S.A., Eisner, P.N., Perez–Cruz, C., 1991. The stratigraphic signatures of tectonics, eustasy and sedimentology – an overview. In: Einsele, G., Ricken, W., Seilacher, A. (Eds.), Cycles and events in stratigraphy. Springer–Verlag, Berlin, pp. 617–659.
Yilmaz, I.O., Hoşgör, I., Mülayim, O., Özer, S., Sarı, B., Tasli, K., 2019. Development of pelagic phase after drowned Arabian Platform, SE Turkey. In: 34th IAS Meeting of Sedimentology Conferences, Roma, Italy, p. 42.
Yılmaz, Y., 1993. New evidence and model on the evolution of the southeast Anatolian Orogen. Bulletin of the Geological Society of America 105, 251–271.
Yılmaz, E., Duran, O., 1997. Güneydoğu Anadolu Bölgesi otokton ve allokton birimler stratigrafi adlama kılavuzu ('Lexicon' guide for stratigraphic nomenclature of the autochthonous and allochthonous units in the southeast Anatolian region). Turkish Petroleum Company, Educational Publication 31, 1–460.

Appendix A. Supplementary data

Supplementary data to this article can be found online at https://doi.org/10.1016/j.cretres.2020.104414.

Appendix

Rudists:	
Durania acuticostata	Caffau et al. (1996)
Sauvagesia sharpei	Bayle (1857)
Caprinula sp.	Choffat (1885)
Ichthyosarcolites monocarinatus	Slišković (1966)
Ichthyosarcolites triangularis	Desmarest (1817)
Bournonia excavata	d'Orbigny (1842)
Bivalve:	
Neithea fleuriausiana	d'Orbigny (1847)
Pithonellid:	
Calcisphaerula innominata	Bonet (1956)
Pithonella ovalis	Lorenz (1902)
Bonetocardiella conoidea	Bonet (1956)
Planktonic foraminifera:	
Asterohedbergella asterospinosa	Hamaoui (1965)
Muricohedbergella planispira	Tappan (1940)